Modulation of proteolysis counteracts oxidative stress but impairs DNA base excision repair in ATM-depleted cells

A thesis presented for degree of Master's by Research in Oncology

Di Yang

Lead supervisor: Prof. Grigory Dianov
Co-supervisor: Prof Tom Brown
Direct supervisor: Dr. Mattia Poletto



St Cross College

CRUK/MRC Oxford institute for Radiation Oncology,
Department of Oncology,
University of Oxford

Michaelmas Term 2017

Acknowledgements

Firstly I would like to appreciate my honour supervisor, Prof. Grigory Dianov (Oncology), and my vice supervisor, Prof. Tom Brown (Chemistry), for providing me the unique opportunity to study within a prestigious laboratory in a preeminent university, working on an intriguing project; I would like to thank Grigory's insightful comments and immense knowledge, and Tom's financial support of my Master study. Secondly I am very grateful to Dr. Mattia Poletto. As the direct supervisor, he has always been inspiring and supportive whenever I had questions and obstacles for the project. I would like to thank for his indispensable experiment ideas, input and patience in providing technical trainings, and valuable suggestions of the thesis. I would also express my gratefulness to other members of the Dianov group: Sally Fletcher, Dr. Arnaud Legrand, Dr. Claudia Grou, Sam Hume and Siobhan Cunniffe—who also provided stimulating discussions and unfailing assistance during the past two years.

Declaration

As this Master project is a collaborated project, I would like to declare that the work presented in this thesis is completely my own. Exceptions are: data mining and representation of SILAC data (**Fig. 3** and **Fig. 7**), and FACS analyses (**Fig. 5** and **Fig. 24**), which were performed by Dr. Mattia Poletto; immunofluorescence analyses (**Fig. 9** and **Fig. 27**) were kindly provided by Dr. Arnaud Legrand.

Word count

17365 words inclusive of legends, in-text citations and references.

Abstract

Ataxia-telangiectasia (A-T), also known as Louis-Bar syndrome, is a neurodegenerative autosomal recessive disease caused by bi-allelic mutations in the ataxia-telangiectasia mutated (ATM) gene. The product of the *ATM* gene is a serine/threonine kinase that acts as primary mediator of cellular signalling pathways in response to various genotoxic stresses, such as DNA damage and reactive oxygen species (ROS). It has been proposed that accumulation of oxidative stress due to loss of functional ATM contributes significantly to the pathogenesis and features of A-T, including neurodegeneration and immunodeficiency. However, despite the severity of the symptoms linked to A-T, lack of functional ATM protein is still compatible with life. We postulated that early adaptive mechanisms must be in place to allow cells to survive in the absence of ATM. Crucially, comprehension of these mechanisms would allow us to elucidate some of the molecular features of A-T, including genomic instability and predisposition to cancer.

To this aim, we adopted a quantitative proteomics approach to study changes occurring early on in normal fibroblasts upon depletion of ATM. We observed that ATM-depleted cells display progressive accumulation of oxidised proteins in the nuclear compartment. Furthermore, our study showed that ATM-depleted cells modulate proteolysis to counteract oxidative stress, which contributes to the survival at early stages after ATM loss. On the other hand, increased proteolysis in ATM-depleted fibroblasts had a negative impact on the frontline DNA repair system counteracting oxidative DNA damage: the DNA base excision repair (BER) pathway. ATM-depleted cells showed lower BER protein levels and severely impaired BER capacity. We propose that DNA repair deficiency caused by BER impairment could be one of the early mechanisms leading to accumulation of genomic instability in ATM-depleted cells.

These previously overlooked adaptation mechanisms give useful insight into the changes occurring very early on upon loss of ATM and provide a molecular explanation for some of the severe features of A-T.

Contents

Contents **5**

List of abbreviations **7**

1. Introduction **8**

1.1 Ataxia-telangiectasia and ATM **8**

1.1.1 Ataxia-telangiectasia: background and diagnosis 8

1.1.2 Ataxia-telangiectasia mutated (ATM) 10

1.1.3 Clinical features of ataxia-telangiectasia 11

1.1.4 Why study the early stages of ATM depletion? 13

1.1.5 Oxidative stress and A-T 14

1.2 DNA Base excision repair pathway (BER) **14**

1.3 Introduction to SILAC proteomics **18**

2. Results **21**

2.1 ATM-depleted fibroblasts display early and progressive accumulation of oxidative stress **21**

2.1.1 ATM-depleted fibroblasts accumulate ROS early on after ATM loss 21

2.1.2 ATM-depleted fibroblasts accumulate oxidised proteins in the nuclear compartment 24

2.2 ATM depletion promotes proteolysis in the nuclear compartment of fibroblasts **26**

2.2.1 ATM-depleted fibroblasts accumulate proteasome subunits in the nucleus 26

2.2.2 Nuclear proteasome subunits in ATM-depleted fibroblasts are fully active 30

2.3 ATM-depleted cells modulate proteolysis to counteract oxidative stress in the nucleus **31**

2.3.1 ROS-generating agents affect localisation of the proteasome 31

2.3.2 Proteolysis is important for survival of ATM-depleted fibroblast 35

2.4 Impaired BER capacity and genomic instability in ATM-depleted cells **39**

2.4.1 BER components are downregulated in ATM-depleted cells 39

2.4.2 Downregulation of BER components is mainly caused by elevated proteolytic activity 40

2.4.3 BER capacity is impaired in ATM-depleted cells 42

2.4.4 ATM-depleted fibroblasts accumulate DNA strand breaks at early stages after ATM loss 50

2.5 The adaptation mechanisms observed in transiently depleted fibroblasts persist in cells obtained from an A-T patient **52**

2.5.1 ..... Cells from an A-T patient exhibit high levels of oxidative stress 52

2.5.2 ..... Proteolysis contributes to survival of A-T cells 54

2.5.3 ..... BER components are downregulated in A-T fibroblasts 57

3. Discussion **58**

3.1 ATM depletion and oxidative stress **59**

3.2 Modulation of proteolysis counteracts oxidative stress and contributes to the survival of ATM-depleted cells 60
3.3 BER impairment and DNA damage in ATM-depleted cells 61
3.3.1 Impaired BER and DNA damage in ATM-depleted cells 61
3.3.2 Is BER deficiency associated with A-T pathogenesis? 62
3.4 Strengths, limitations and conclusions of this study 63
3.4.1 Strengths and limitations of our approach 63
3.4.2 Conclusions 64
4. Material and methods 66
4.1 Materials 66
4.1.1 Table list of antibodies 66
4.1.2 Table list of oligonucleotide sequences 66
4.2 Methods 67
4.2.1 Cell culture and siRNA transfections 67
4.2.2 Stable isotope labelling with amino acids in cell culture (SILAC) and mass spectrometry . 68
4.2.3 Generation of cell extracts 68
4.2.4 Sodium dodecyl sulphate polyacrylamide gel electrophoresis (SDS-PAGE) and Western blot 69
4.2.5 Detection of protein carbonylation 70
4.2.6 Immunostaining 70
4.2.7 *In vitro* proteasome and BER assays 71
4.2.8 Comet assays 73
4.2.9 Statistical analyses 74
References 75

List of abbreviations

53BP1	p53-binding protein 1
5’ dRP	5’ deoxyribose-phosphate
AMPK	AMP–activated protein kinase
AP	Apurinic/apyrimidinic
APE1	Apurinic/apyrimidinic endonuclease 1
A-T	Ataxia-telangiectasia
ATM	Ataxia telangiectasia mutated
BRCA1	Breast cancer type 1 susceptibility protein
BER	Base excision repair
Chk2	Checkpoint kinase 2
DDR	DNA damage response
DMEM	Dulbecco's Modified Eagle's Medium
DMSO	Dimethylsulphoxide
DNPH	2,4-dinitrophenylhydrazine
DSBs	DNA double strand breaks
DTT	Dithiothreitol
EDTA	Ethylenediaminetetraacetic acid
FACS	Fluorescence-activated cell sorting
FBS	Foetal bovine serum
FEN1	Flap endonuclease 1
GSTs	Glutathione S-transferases
H2DCFDA	2',7'-dichlorodihydrofluorescein diacetate
HRR	Homologous-recombinant repair
LigIII	DNA ligase 3
MAP	Mitogen activated protein
MMS	Methyl Methanesulfonate
MRN	Mre11-Rad50-Nbs1
NAC	N-acetyl cysteine
NEM	N-ethylmaleimide
NHEJ	Non-homologous end-joining
PBS	phosphate-buffered saline
PCNA	Proliferating cell nuclear antigen
PCV	Packed cell volume
PI3Ks	Phosphatidylinositol 3-kinases
PMSF	Phenylmethanesulfonyl fluoride
PNKP	Polynucleotide kinase-phosphatase
POLβ	DNA Polymerase β
POLδ	DNA Polymerase δ
PQ	Paraquat
PRDXs	Peroxiredoxins
PVDF	Polyvinylidene fluoride
ROS	Reactive oxygen species
SDS	Sodium dodecyl sulphate
SDS-PAGE	Sodium dodecyl sulphate polyacrylamide gel electrophoresis
SILAC	Stable isotope labelling with amino acids in cell culture
siRNA	Small interfering RNA
SSBs	Single strand breaks
TBE	Tris/borate/EDTA
TG	Tris/glycine
TGS	Tris/glycine/SDS
THF	Tetrahydrofuran
WCEs	Whole cell extracts
XRCC1	X-ray repair cross complementing 1

1. Introduction

Ataxia-telangiectasia (A-T) is a rare autosomal recessive disease caused by mutations in the ataxia-telangiectasia mutated (*ATM*) gene, which encodes for a serine/threonine-specific protein kinase involved in mediating the coordination of cellular signalling pathways in response to genotoxic stress. A-T is characterised by multi-systemic features, including progressive neurological impairment, cerebellar ataxia, immunodeficiency and hypersensitivity to ionising irradiation. Importantly, the disease is associated with persistent oxidative stress, which has been proposed to be an underlying cause of the broad spectrum of symptoms. Oxidative stress, due to unbalanced homeostasis of reactive oxygen species (ROS), can lead to oxidative DNA damage. The DNA base excision repair (BER) pathway is the frontline DNA repair pathway responsible for the clearance of ROS-induced DNA damage. Although a number of studies suggest the existence of a crosstalk between ATM and BER, it is still unclear if BER is affected in the absence of a functional ATM protein.

In the following paragraphs I will introduce the main features of A-T and describe the functions of ATM. Then, the BER pathway and the relationship between ATM and BER will be introduced, with particular emphasis on the potential role of this connection in A-T pathogenesis. Moreover, I will briefly describe the quantitative proteomics approach adopted by the laboratory to understand the adaptation mechanisms arising in the absence of ATM, which was the starting point of my project.

1.1 Ataxia-telangiectasia and ATM

1.1.1 Ataxia-telangiectasia: background and diagnosis

A-T, which is also known as Louis-Bar Syndrome, is a rare, neurodegenerative, autosomal recessive form of cerebellar ataxia (Anhei et al., 2012). The disease was first documented by Syllaba and Henner in 1926 (Syllaba & Henner, 1926), who reported the observation of progressive

choreoathetosis and ocular telangiectasia in three siblings from the same family. Despite the fact that Louis-Bar published a paper describing a Belgian patient with progressive cerebellar ataxia and cutaneous telangiectasia in 1941 (Louis-Bar, 1941), A-T was not documented as an individual clinical entity until 1957, when Boder and Sedgwick characterised the major features of this familial syndrome upon reanalysis of the three siblings described in Syllaba and Henner's report (Sedgwick & Border, 1960).

A-T is identified as a syndrome of cerebellar ataxia. It is caused by bi-allelic mutations in the *ATM* gene, which encodes for a kinase that acts as the key regulator of cellular response to genotoxic stress (see section 1.1.2) (Swift et al., 1986). Ataxia is a non-specific clinical manifestation of muscle incoordination, which includes wobbly gait, swallowing difficulties and other abnormalities caused by lack of voluntary coordination of muscle movements (Savitsky et al., 1995). This implies a dysfunction of parts of the brain coordinating movements, typically the cerebellum. Ataxia is usually the first indication of A-T, which occurs in toddlers. When patients start walking, they manifest difficulty in standing still and show a characteristic wobbly gait (Schmahmann, 2004) (Hoche et al., 2012). The situation usually degenerates when the patients reach their second decade, as reading becomes increasingly difficult due to the defect in coordinating eye movement (Crawford et al., 2000). The term "telangiectasia" highlights the emergence of small dilated blood vessels appearing near the skin surface (Chussil, 1992). In the case of A-T, telangiectasia usually occurs over the sclera around 5-8 years of age, even though it does not necessarily appear in all A-T cases (Cabana et al., 1998).

Individuals affected with A-T often develop symptoms with variable severity at different ages. However, A-T cannot usually be confirmed before school age, when symptoms start to develop or worsen (Rothblum-Oviatt et al., 2016). In addition to the combination of neurological features and telangiectasia, A-T can be diagnosed in the laboratory (Sun et al., 2002) (Chun et al., 2003). This is

done, for example, by assessing the absence or deficiency of ATM protein in blood cells taken from the patient.

1.1.2 Ataxia-telangiectasia mutated (ATM)

About 22 years ago, Savitsky et al. reported for the first time that mutation of a single gene, named *ATM*, was the fundamental cause of A-T (Savitsky et al., 1995). As A-T is a multi-systemic disease, the identification of a single responsible gene was a great breakthrough in understanding the molecular basis underlying the pathology (Nowak, 1995). The *ATM* gene encodes for a large protein (approx. 350kDa) that shares sequence similarity with the lipid kinase family phosphatidylinositol 3-kinases (PI3Ks). ATM is in fact a serine/threonine-specific protein kinase (Shiloh & Ziv, 2013). Currently, more than 300 disease-causing mutations occurring throughout the *ATM* gene have been documented (Broeks et al., 2000). Most of these lead to premature truncation of the protein product and protein instability (Natalia et al., 1999) (Lakin et al., 1996). Some of the mutations lead to decreased amount of functional protein or normal amount of protein with dramatically reduced kinase activity (Savitsky et al., 1995).

ATM is a master regulator of a number of cellular signalling pathways in response to multiple kinds of stress (Shiloh & Ziv, 2013) (Stracker et al., 2013) (Paull, 2015). The best studied function of ATM is related to the activation and coordination of cellular signalling pathways in response to DNA double strand breaks (DSBs). Upon induction of DSBs, ATM is recruited by the Mre11-Rad50-Nbs1 (MRN) complex to the sites of damage and undergoes auto-phosphorylation at serine 1981. This phosphorylation event causes conformational changes that expose the normally inaccessible carboxy-terminal active site, leading to full activation of the protein's kinase activity and subsequent phosphorylation of a series of downstream effectors. Most of these effectors, such as check kinase 2 (Chk2) and tumour suppressor p53, phosphorylate or transcriptionally activate other proteins

involved in the DNA damage response, resulting in a finely tuned coordination between DNA repair and cell cycle (Lee & Paull, 2005) (Matsuoka et al., 2000).

ATM kinase activity is critical to cells, as it enforces cell cycle checkpoints and allows additional time for DNA repair before DNA lesions such as DNA single strand breaks (SSBs) are converted to DSBs, which are a threat to genome stability. In support of this idea, recent data from our laboratory have shown that ATM can be also activated by endogenous DNA damage in the absence of detectable DSBs (Khoronenkova & Dianov, 2015). These data suggest that other kinds of DNA lesions - in addition to DSBs - (e.g. SSBs) can be sensed by the kinase.

In addition to act as a direct sensor for DNA damage, activation of the protein has been suggested to occur in response to oxidative stress (Guo, Deshpande, & Paull, 2010) (Guo et al., 2010) (Kozlov et al., 2016). In the presence of ROS, activated ATM has been shown to phosphorylate other kinases, including AKT and AMP-activated protein kinase (AMPK). This has been suggested to counteract oxidative stress, as these kinases can affect multiple signalling pathways that downregulate energy-consuming and oxidative metabolisms (e.g. DNA replication, cell proliferation, aerobic respiration…) to reduce intracellular oxidative load. At the same time, the same pathways can trigger autophagy as well as antioxidant defence mechanisms, to scavenge ROS (Alexander et al., 2010) (Khalil et al ., 2012).

1.1.3 Clinical features of ataxia-telangiectasia

A-T is a rare disease., Its incidence is estimated to vary from 1 in 40,000 to 1 in 100,000 live births (Swift et al., 1986). The main causes of death in A-T patients are lung infections (about one-third) and cancer (about one-third) (Rothblum-Oviatt et al., 2016). Although the disease is primarily caused by mutations in a single gene, it should not come as a surprise that A-T patients display a wide range of clinical manifestations, as ATM acts a master regulator for a number of distinct signalling pathways.

The most severe clinical feature associated with A-T is progressive neurodegeneration, mainly resulting from cerebellar atrophy (Gilmore, 2014). Based on abnormalities observed in cells lacking ATM, several hypotheses have been put forward to explain the cause of neurological cell death (Herzog et al., 1998) (Biton et al., 2008) (Valentin-Vega et al., 2012). The exact mechanism is, however, still poorly understood. Another devastating feature of A-T is immunodeficiency, which occurs in two third of the patients (Nowak-Wegrzyn et al., 2004). The major A-T-related immunological manifestations include dramatically decreased levels of immunoglobulins (especially the IgA and IgG sub-classes), sinopulmonary infections (Nowak-Wegrzyn et al., 2004) and lymphopenia (Driessen et al., 2013). ATM has been shown to regulate V(D)J recombination during the production of immunoglobulins (Bredemeyer et al., 2006), as well as proliferation of T cells (Bagley et al., 2007). In the absence of ATM, prompt activation of T cells and generation of antibodies in response to a specific antigen are potentially aborted, which may explain why most A-T patients have a defective immune system.

In addition to neurodegeneration and immunodeficiency, hypersensitivity to ionising radiation is another hallmark of A-T. Radiosensitivity was observed in A-T patients subjected to radiotherapy (Feigin et al., 1970) (Morgan et al., 1968) and confirmed *in vitro* on A-T leukocyte cell cultures after radiation exposure (Higurashi & Conen, 1973). As explained above, ATM is responsible for activation of cell cycle check points in response to DNA damage (Matsuoka et al., 2000). Therefore, A-T cells are likely unable to properly repair radiation-induced DNA damage. This could explain hypersensitivity of A-T cells to ionising radiation. Moreover, accumulation of DNA damage may result in genomic instability, causing predisposition to cancer typically observed in A-T patients (Gatti et al., 1991) (McKinnon, 2004) (Savitsky et al., 1995).

Although A-T occurs with low frequency, understanding the mechanisms at the basis of the disease is of great interest for a number of reasons: clearer comprehension of A-T not only will improve management of patients, but also could potentially shed light on the pathogenesis of a broader

spectrum of diseases (e.g. neurodegenerative conditions and cancer). Besides, learning more about ATM constitutes an invaluable opportunity to study in depth the molecular mechanisms underlying the DNA damage response.

1.1.4 Why study the early stages of ATM depletion?

While no cure for A-T is currently available, palliative care can bring the average life expectancy of a patient to 25 years and beyond (Rothblum-Oviatt et al., 2016) (Crawford et al., 2006). The puzzling aspect of A-T is that, despite the severity of phenotypes and the diversity of symptoms linked with A-T, loss of functional ATM is still compatible with life. Therefore, we hypothesise that there must be a number of adaptive mechanisms that allow survival of cells during embryonic development and through adulthood in the absence of ATM. As mentioned earlier, the phenotype of cells lacking ATM has been extensively characterised. However, most of the studies carried out so far have made use of cells derived either from A-T patients or from knock-out mouse models. Nonetheless, we have to consider that A-T is a genome instability syndrome (Shiloh & Kastan, 2001). Cells derived from A-T patients and ATM knock-out mice have been reported to be genetically unstable (Shiloh, 2003) (Barlow et al., 1996). In theory, cell models traditionally used to study A-T could potentially establish chromosomal rearrangements during long-term propagation in culture. For this reason, their phenotype is likely to vary with the accumulation of chromosomal alterations.

In this thesis, we postulate that the phenotypical changes that occur early on following loss of ATM could be masked by phenomena indirectly arising as a consequence of genetic instability. Therefore, it is possible that early changes in cells lacking ATM might have been overlooked in previous studies. To address this issue, in this thesis we analyse the phenotypic changes occurring in normal human embryonic fibroblasts (TIG-1 cells) early on upon transient siRNA-mediated depletion of ATM.

1.1.5 Oxidative stress and A-T

It is very important to highlight that A-T pathogenesis has been extensively linked to persistent oxidative stress. Elevated levels of ROS have been documented both in cells derived from the cerebellum of ATM knockout mice (Kamsler et al., 2001) and in lymphocytes obtained from A-T patients (Reichenbach et al., 2002). Importantly, it has been suggested that persistent oxidative stress could contribute largely to the broad spectrum of symptoms associated with the A-T syndrome (D'Souza et al., 2013) (Rotman & Shiloh, 1997) (J Reichenbach et al., 1999). For example, neuronal cells are highly metabolic, they require a great amount of oxygen to synthesise ATP to support their function; therefore, these cells are thought to be particularly prone to generation of oxidative stress (Lin & Beal, 2006) (Uttara et al., 2009). As mentioned earlier, ATM is involved in the maintenance of ROS homeostasis. In the absence of ATM, neuronal cells are constantly exposed to unbalanced ROS production, which can cause cell death by activating the mitogen activated protein (MAP) kinase cascade and eventually lead to A-T associated neuronal dysfunction (Uttara et al., 2009).

Interestingly, administration of antioxidants such as N-acetyl cysteine (NAC) to ATM knockout mice has been shown to restore aberrant V(D)J recombination and normal T cell development, improving immunodeficiency and delaying the onset of thymic lymphoma (Ito et al., 2007). These observations further suggests that impaired response to oxidative stress in the absence of functional ATM might be a major underlying cause of A-T, leading to immunological deficiency and cancer propensity in A-T animals, and likely in A-T patients.

1.2 DNA Base excision repair pathway (BER)

BER is the frontline DNA repair pathway mediating the elimination of small lesions arising in the genome as a result of oxidation or alkylation of DNA (Lindahl, 2000) (Dianov & Hübscher, 2013). The

pathway plays an important role in protecting cells from DNA damage and genomic instability (Maynard at al., 2009). This thesis will extensively deal with oxidative damage and with the relationship between ATM, A-T and BER. For this reason, I will provide here a brief introduction about the BER pathway.

Oxidative stress and unbalanced generation of ROS, can cause extensive damage to cellular macromolecules such as DNA, proteins and lipids (Avery, 2011) (Schieber & Chandel, 2014). As a by-product of normal oxygen metabolism, ROS can not only damage nucleotides and lead to DNA lesions, but also react with the sugar-phosphate backbone to directly generate DNA strand breaks (Melvin et al., 1996). These oxidative lesions must be repaired promptly to prevent development of genome instability. To defend the genome from DNA damage, cells have evolved an array of DNA repair pathways that efficiently clear specific types of lesions. BER is the primary DNA repair pathway responsible for removing oxidative DNA damage (Cooke et al., 2003) (Maynard et al., 2009). Importantly, most of the lesions the pathway deals with are of endogenous origin and arise spontaneously at a considerable rate every day in every cell (Lindahl, 1993); therefore BER plays crucial role in maintaining genome integrity by removing any DNA lesions generated endogenously before mutations are fixed into the genome.

The BER pathway is a coordinated process involving a number of enzymes, which identify and eliminate the specific DNA lesion and mediate the synthesis of an intact strand of DNA (Fig. 1). The first step of BER involves the recognition and removal of the damaged base by a DNA glycosylase, which generates an apurinic/apyrimidinic site (AP site) (Seeberg et al., 1995). In mammalian cells, the AP endonuclease APE1 subsequently incises the sugar-phosphate backbone at the AP site and generates a SSB (Chen et al., 1991) (Sung & Demple, 2006). To allow synthesis and ligation of the incised DNA strand, the DNA strand break must possess a 3'-hydroxyl and a 5'-phosphate group. This is ensured by "end-trimming" enzymes such as polynucleotide kinase-phosphatase (PNKP), which promote 5'-phosphorylation and removes phosphates from 3' DNA ends (Chen et al., 1991).

The SSB originating from APE1 incision can be processed by two BER sub-pathways: the short-patch and long-patch BER. As illustrated in Fig. 1, different players are respectively involved in the two mechanisms. The protein X-ray repair cross complementing 1 (XRCC1) is one of the core BER components recruited to the nick at the AP site. While XRCC1 has no known enzymatic activity, the protein functions as an important scaffold protein that coordinates the short-patch BER (Robertson et al., 2009). XRCC1 interacts with DNA polymerase β (POLβ) and DNA ligase 3 (LigIII) to facilitate the insertion and ligation of a single nucleotide, and to promote the removal of the 5' deoxyribose-phosphate (5' dRP) generated in the short-patch BER pathway (Cappelli et al., 1997). Conversely, the long-patch BER pathway is dependent on the nuclear protein proliferating cell nuclear antigen (PCNA) (Robertson et al., 2009) (Frosina et al., 1996). PCNA interacts with and promotes the enzymatic activity of DNA polymerase δ (POLδ) and Flap endonuclease 1 (FEN1). POLδ can perform strand displacement synthesis of the new DNA strand and promotes cleavage of the displaced DNA "flap" by FEN1, before the nick can be ligated in a way similar to the short-patch BER (Kim et al., 1998).

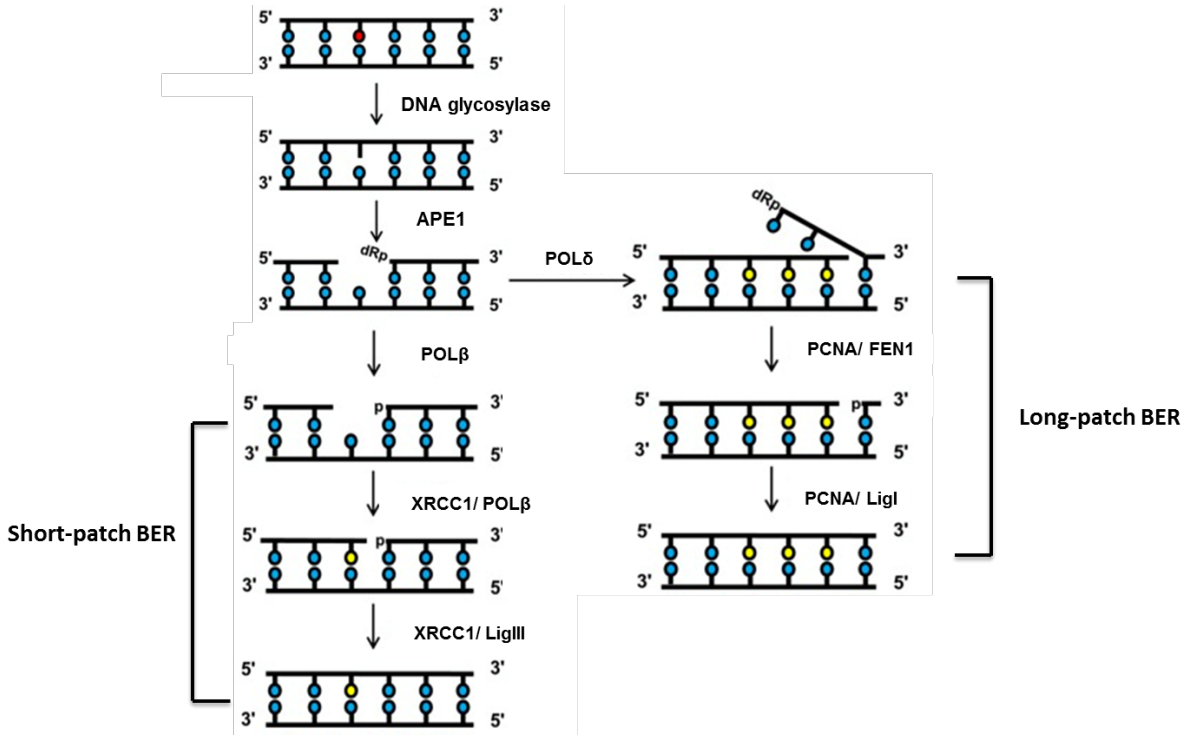


Fig.1 DNA base excision repair. A DNA glycosylase specifically recognises and removes the DNA base lesion, resulting in an AP site. APE1 cleaves at the AP site and subsequently generates a nick which can be processed by two different BER sub-pathways. Adapted from (Nickson & Parsons, 2014).

As introduced earlier, ATM is conventionally regarded as a DSB sensor. Nonetheless, recent reports have suggested that its kinase activity can also be activated by other endogenous forms of DNA damage such as DNA SSBs, R-loops and A-P sites (Sordet et al., 2009) (Khoronenkova & Dianov, 2015). As loss of functional ATM has been widely linked to induction of oxidative stress, it is tempting to speculate that BER could have a leading role in DNA repair in the absence of ATM. Previous studies not only have suggested a crosstalk existing between BER and the ATM-mediated DNA damage response (DDR) (Chou et al., 2015), but also hint at potential roles played by BER in the context of A-T.

DNA repair pathways in A-T cells are, in general, poorly characterised. In light of a potential relevance between BER and A-T pathogenesis, it would be intriguing to investigate the impact of ATM depletion on the BER pathway. In this thesis, I will discuss how loss of ATM can affect BER and how this could explain some of the molecular features of A-T.

1.3 Introduction to SILAC proteomics

This thesis project stemmed from a proteome-wide analysis carried out in our laboratory on normal human fibroblasts (TIG-1 cells) transfected with an ATM-targeting siRNA. The lab made use of a quantitative proteomics approach known as "stable isotope labelling with amino acids in cell culture (SILAC)" and displayed in Fig. 2. SILAC is a mass spectrometry-based technique that quantitatively detects differences in protein abundance between samples using non-radioactive isotopic labelling (Ong et al., 2002) (Mann, 2006) (Oda et al., 1999). As illustrated in Fig. 2, two groups of samples (in this case cells treated with a control siRNA - siCtrl and cells treated with an ATM-targeting siRNA - siATM) were fed with either regular, unlabelled medium (R_0K_0) or medium containing amino acids labelled with "heavy" isotopes ($R_{10}K_8$). As a result, proteins from siATM-treated cells incorporated "heavy" amino acids (i.e. arginine and lysine), while proteins synthesised in siCtrl-treated cells did not. Seventy-two hours post-transfection siCtrl and siATM cells were harvested and mixed in a 1:1 ratio. Cytoplasmic and nuclear protein extracts were generated from mixed cells, and digested into peptides. Samples were then analysed using mass spectrometry (See section 4.2.2). In this way, changes in the abundance of chemically identical peptides could be detected according to the mass difference due to differentially incorporated amino acids in individual samples. Fractionation into nuclear and cytoplasmic compartments allowed us to maximise the coverage of the analysis. Additionally, this gave us some insight into the subcellular localisation of proteins of interest in response to ATM depletion.

By analysing the SILAC data, we observed a remarkable difference between the proteome of siCtrl and siATM cells. It was very interesting to observe a widespread upregulation of a number of proteins responsible for maintaining cellular redox homeostasis in ATM-depleted cells (Fig.3). These included peroxiredoxins (PRDXs), a family of ubiquitous anti-oxidant enzymes that are responsible for eliminating free peroxides (Winterbourn, 2013), and proteins belonging to the glutathione S-transferase family (GSTs), which are responsible for catalysing the conjugation of reduced

glutathione to xenobiotic molecules for the purpose of detoxification (Jakoby, 1978). These observations were in line with previous studies demonstrating accumulation of oxidative stress in A-T cells (see section 1.1.5).

The proteomics study carried out in the lab suggested a strong contribution of oxidative stress to the early response to a loss of ATM. Moreover, remarkable protein expression changes were detected for proteasome components. These observations will be thoroughly discussed in the following chapters.

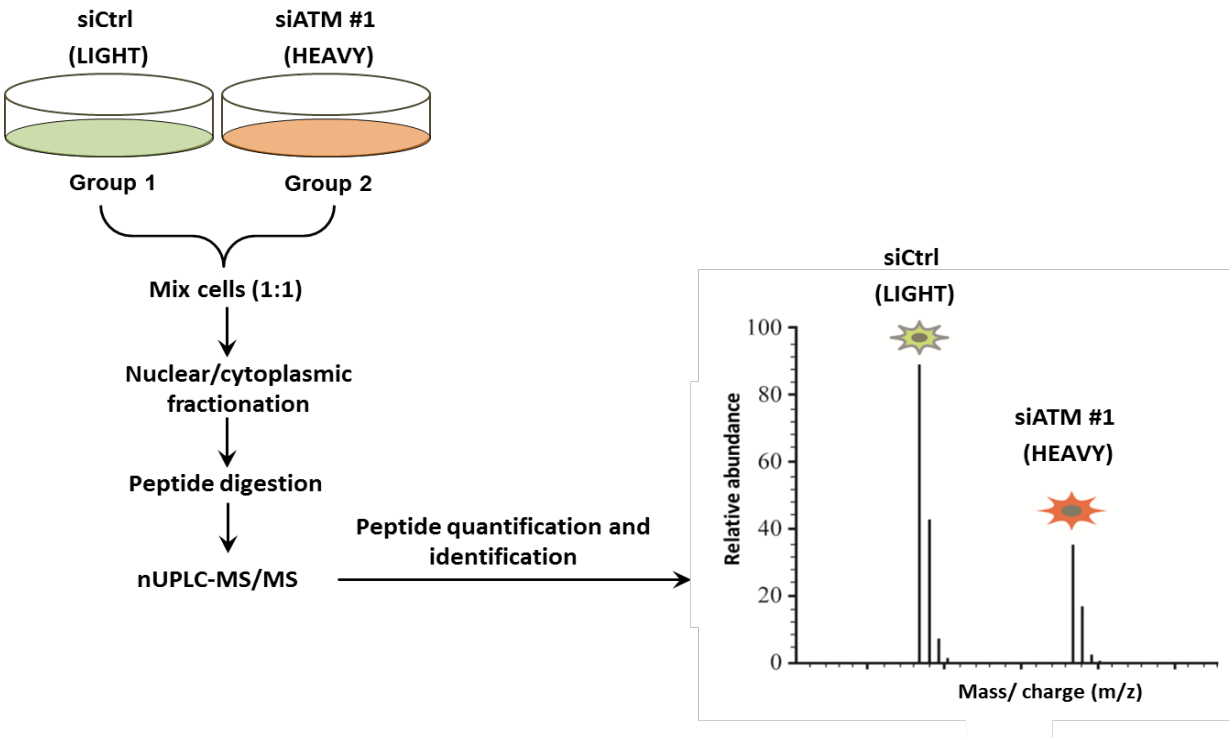


Fig.2 Schematic diagram illustrating the SILAC technique. Two groups of cells were fed with either the "light" (R_0K_0) or the "heavy" ($R_{10}K_8$) culture medium. 72 hours post transfection proteins were extracted from a 1:1 cell mixture and digested into peptides by trypsin. Samples were analysed by a nano-ultraperformance liquid chromatography tandem mass spectrometry (nUPLC-MS/MS), the relative abundance of different peptide species was calculated according to the mass difference.

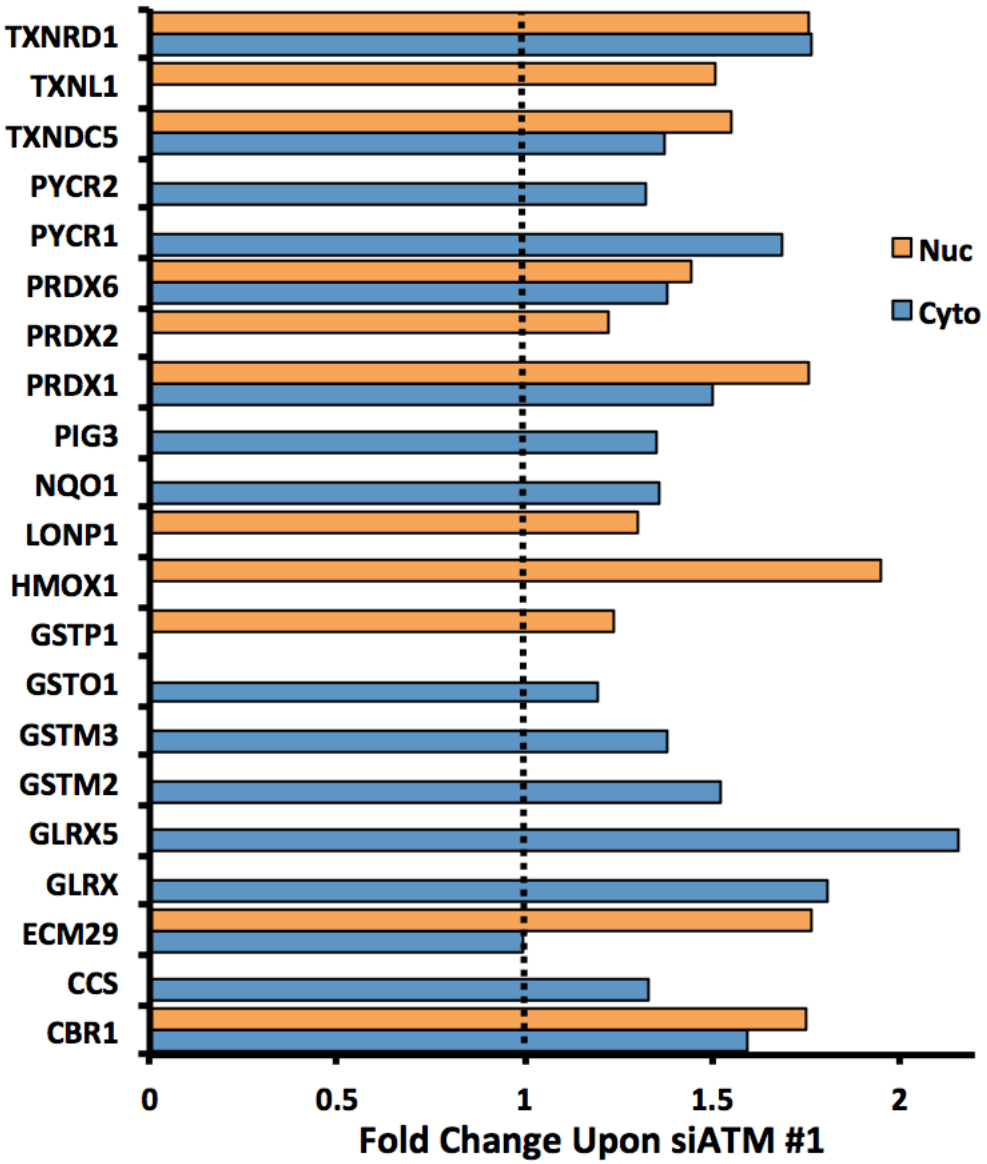


Fig.3 Histogram illustrating the relative abundance of proteins involved in the antioxidant response in nuclear and cytoplasmic cell extracts obtained from ATM-depleted cells (siATM). The data shown in the graph are expressed as fold of change of protein levels in ATM-depleted cells normalised to cells transfected with a control siRNA (dashed line). Orange and blue bars indicate protein levels in the nuclear and cytoplasmic compartments, respectively.

2. Results

2.1 ATM-depleted fibroblasts display early and progressive accumulation of oxidative stress

2.1.1 ATM-depleted fibroblasts accumulate ROS early on after ATM loss

As suggested by our proteomics analysis, ATM-depleted cells upregulate genes involved in the regulation of redox homeostasis (Fig. 3). In fact, as ATM has been recently proposed to act as a sensor for ROS (Guo, Deshpande, et al., 2010), activation of antioxidant genes could be induced by increased level of cellular ROS in cells lacking ATM (Espinosa-Diez et al., 2015). We validated this hypothesis by measuring the levels of intracellular ROS in ATM-depleted cells by using a fluorescent probe (2',7'-dichlorodihydrofluorescein diacetate - H2DCFDA). Fluorescence of H2DCFDA was assessed using fluorescence-activated cell sorting (FACS), in a time-course experiment of ATM depletion. As early as thirty-six hours after transfection of the ATM-specific siRNA, ATM protein levels showed downregulation when compared with the control siRNA-treated fibroblasts (Fig. 4). Consistently, significant accumulation (1.2 fold) of ROS content occurred as early as thirty-six hours after transfection (Fig. 5). ROS levels rose to 2.2 fold in ATM-depleted cells seventy-two hours post-transfection. At this time point, the amount of ROS induced by ATM depletion was comparable to that obtained treating cells with 25 μM H_2O_2 (Fig 5). These observations are in accordance with the gradual loss in ATM showed in Fig. 4. Our data confirm previous reports suggesting that cells lacking ATM exhibit elevated levels of ROS (Barzilai et al., 2002) (Kamsler et al., 2001) (Reichenbach et al., 2002). Moreover, the data show here for the first time that the increase in intracellular ROS levels is a very early event occurring after loss of ATM.

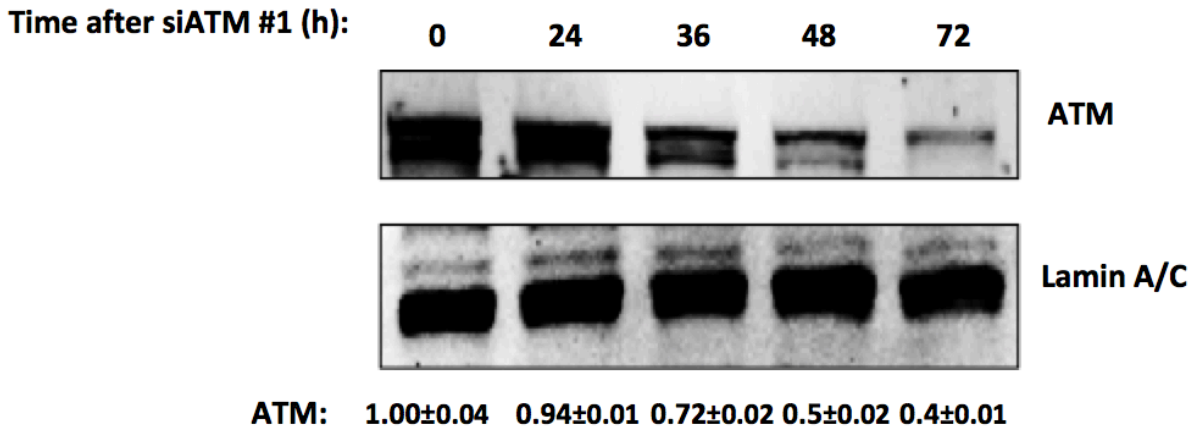


Fig.4 Representative Western blot image of a time-course experiment of ATM depletion. TIG-1 fibroblasts were harvested at the indicated time post-transfection with either a control siRNA (siCtrl) or a siRNA targeting ATM (siATM). 25µg of nuclear extracts were loaded on an 8% polyacrylamide gel. Lamin was used as loading control. Densitometric quantification of ATM (with the mean ± SD from three independent experiments) is reported at the bottom.

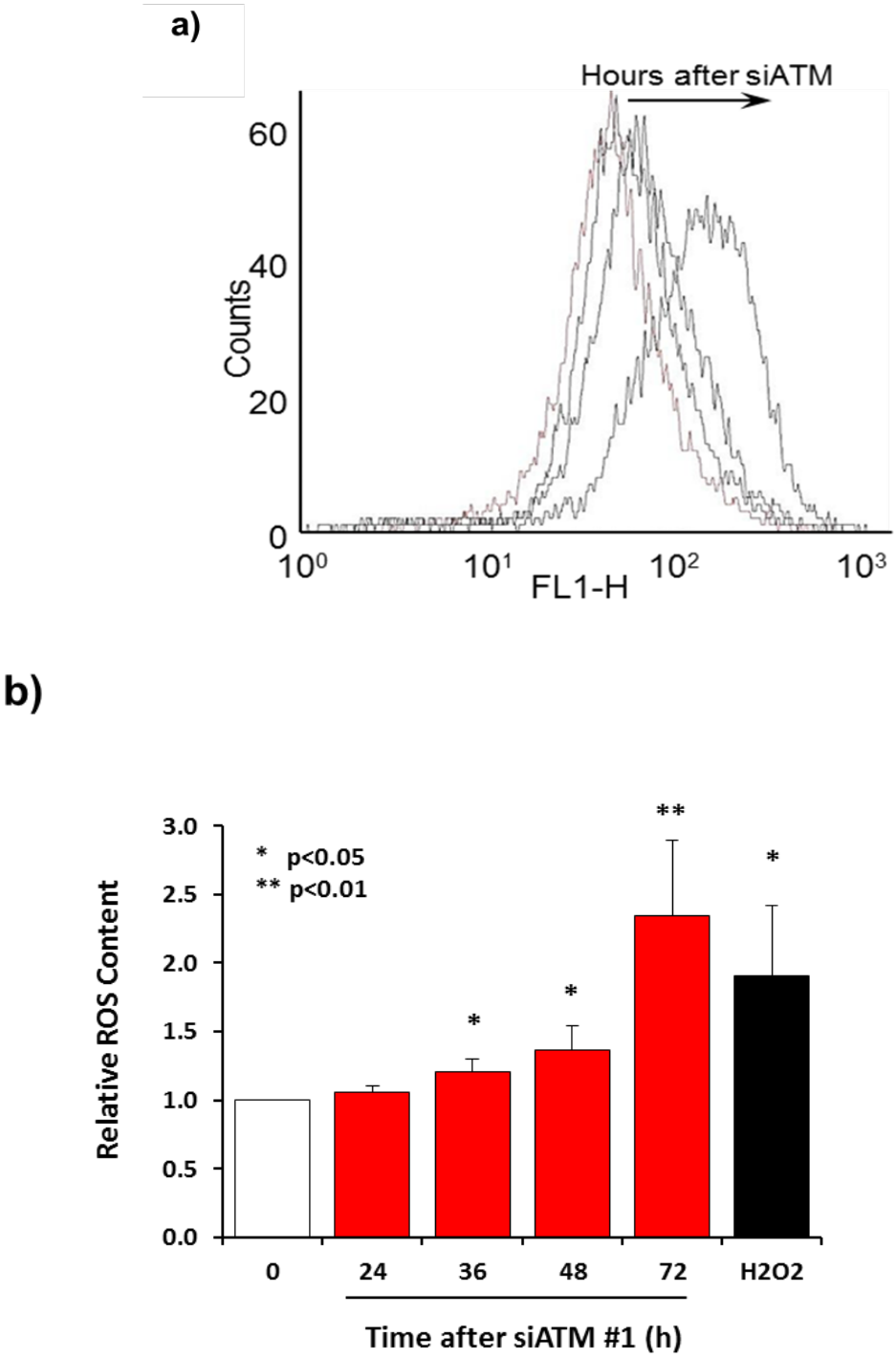


Fig.5 a) Flow-cytometry assay to detect intracellular ROS content. **a)** Representative histogram showing how ATM-depleted fibroblasts accumulate ROS progressively with time (24, 48 and 72 hours) of transfection. The Y-axis reports the fluorescence intensity of the probe, reflecting ROS levels. The greater the fluorescence intensity, the higher the ROS content. **b)** Quantification of ROS content in **a)**. The histogram was generated by quantifying the relative change in fluorescence intensity compared to untransfected cells. Cells treated with 25µM H_2O_2 for 30 min were used as a positive control. Data was obtained from three independent experiments. (* $p<0.05$, ** $p<0.01$).

2.1.2 ATM-depleted fibroblasts accumulate oxidised proteins in the nuclear compartment

ROS can oxidise protein molecules in different ways; protein carbonylation is one of the major oxidative modifications induced by ROS (Davies, 2016). Side chains of amino acids such as lysine, proline and threonine can be directly oxidised by ROS and result in 2,4-dinitrophenylhydrazine (DNPH)-detectable carbonylated products (Suzuki et al., 2010). The level of carbonyl groups in proteins is widely accepted as a biomarker for oxidative protein damage; this is mainly due to its relative early formation and stability (Beal, 2002) (Dalle-Donne et al., 2003). As we observed time-dependent accumulation of ROS in ATM-depleted fibroblasts, we assayed by Western blot the level of oxidised proteins over a time course similar to the one shown in Fig 4. Cell extracts were incubated with DNPH, and DNPH-derivatised proteins were then separated by polyacrylamide gel electrophoresis. Western blot with an antibody specifically recognising the DNP moiety allowed us to assess the amount of oxidised proteins. Consistent with the progressive increase in ROS content (Fig. 5), we observed a time-dependent accumulation of oxidised proteins seventy-two hours after ATM depletion (Fig.6). This occurred consistently in the nuclear compartment of ATM-depleted fibroblasts, less so in the cytoplasmic fraction (not shown).

Our data indicate that ATM-depleted fibroblasts start to accumulate oxidative stress very early on after ATM loss. While this phenotype is consistent with previous observations in A-T patient cells and cells derived from ATM knockout models, we show here for the first time that proteins in ATM-depleted cells accumulate oxidative modifications.

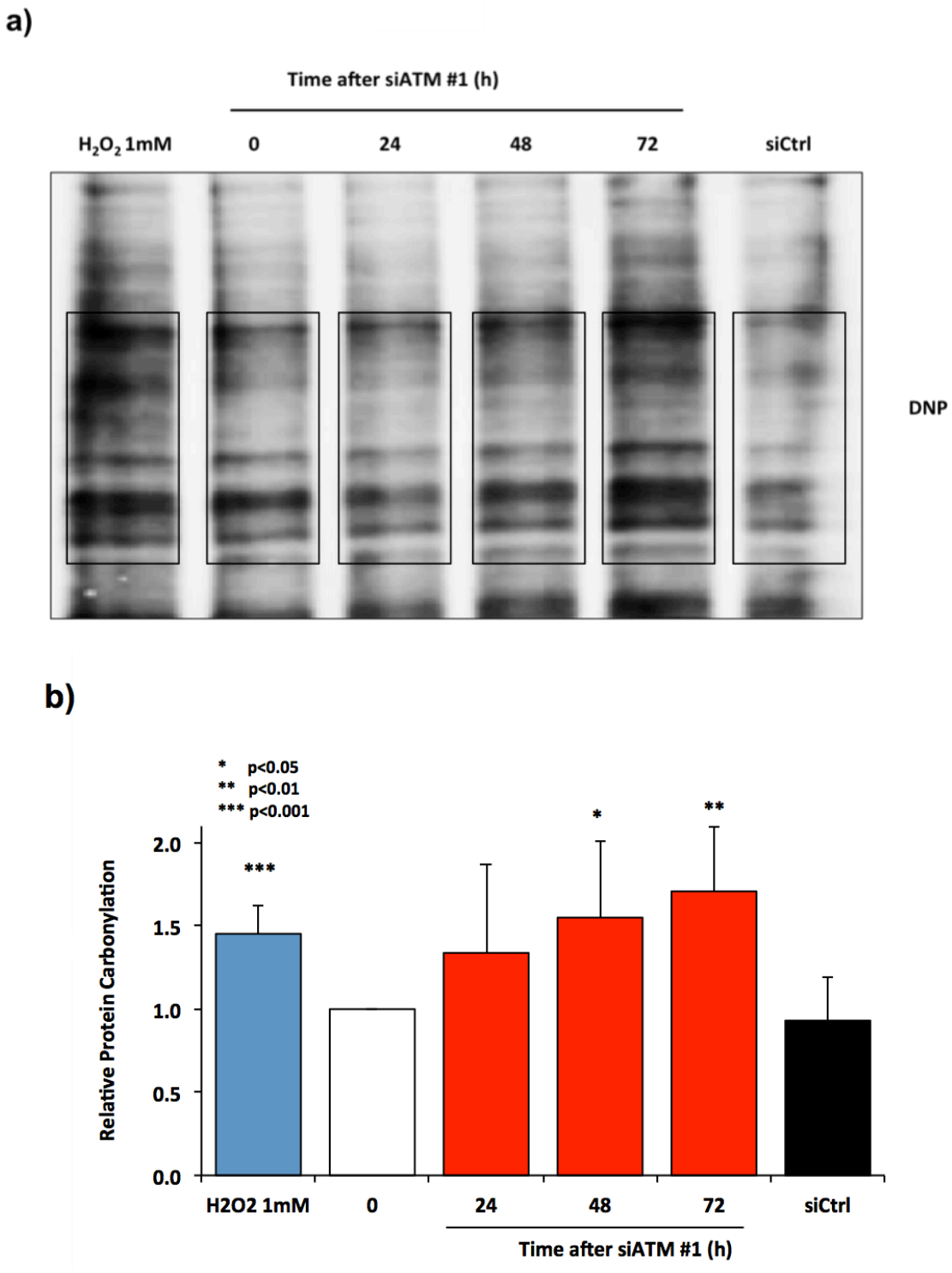


Fig.6 a) Representative Western blot image of carbonylated proteins in the nuclear compartment of fibroblasts transfected with either siCtrl or siATM. Cells treated with 1 mM H_2O_2 for 30 min were used as a positive control. 10 µg of nuclear extracts were loaded on an 8% polyacrylamide gel. Black boxes indicate regions that were used for quantification. **b)** Densitometric quantification of carbonylated proteins in **a).** (* p<0.05, ** p<0.01, *** p<0.001).

2.2 ATM depletion promotes proteolysis in the nuclear compartment of fibroblasts

2.2.1 ATM-depleted fibroblasts accumulate proteasome subunits in the nucleus

As showed in section 2.1.2, extensive oxidative stress can cause accumulation of oxidised proteins, which tend to cluster into non-functional aggregates (Tyedmers et al., 2010). In humans, protein homeostasis is maintained by the ubiquitin-proteasome-system (UPS), and misfolded and damaged proteins are degraded through a proteolytic machinery, the 26S proteasome (Lecker et al., 2006). The 26S proteasome is a multi-subunit protein complex constituted of a 20S catalytic core and a pair of 19S regulatory particles (Voges et al., 1999). Interestingly, our SILAC analysis highlighted a remarkable upregulation of several proteasomal subunits, specifically occurring in the nuclear compartment of ATM-depleted cells (Fig. 7). We hypothesised that accumulation of the proteasome in the nuclear compartment could be a protective mechanism triggered by ATM-depleted cells in order to counteract oxidative protein damage.

First, we validated our proteomic data by performing a series of experiments in fibroblasts depleted of ATM by means of different ATM-targeting siRNAs. A subset of the proteasome subunits was selected for the analysis. These included the regulatory subunit PSMD13 and two subunits constituting the catalytic core of the 26S proteasome, namely PSMA5 and PSMB5. We observed by Western blot a significant increase in the amount of PSMD13, PSMA5 and PSMB5 in nuclear, but not cytoplasmic extracts obtained from cells transfected with either ATM-targeting siRNA (Fig. 8). Consistent with these results, immunofluorescence assays also confirmed the results obtained from the proteomics analysis, showing a 3-3.25 fold increase in the nuclear levels of PSMD13 in ATM-depleted fibroblasts (Fig. 9).

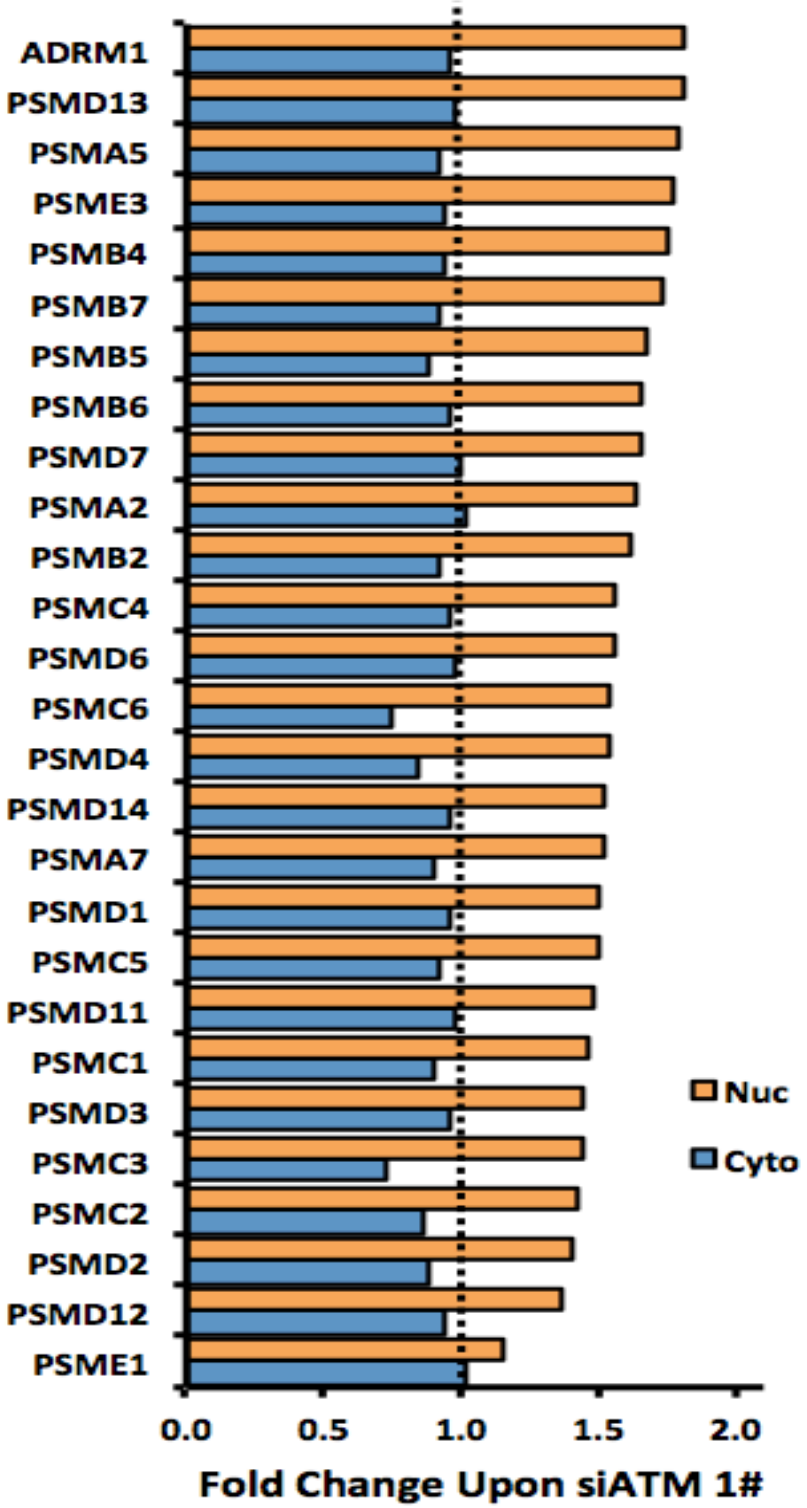
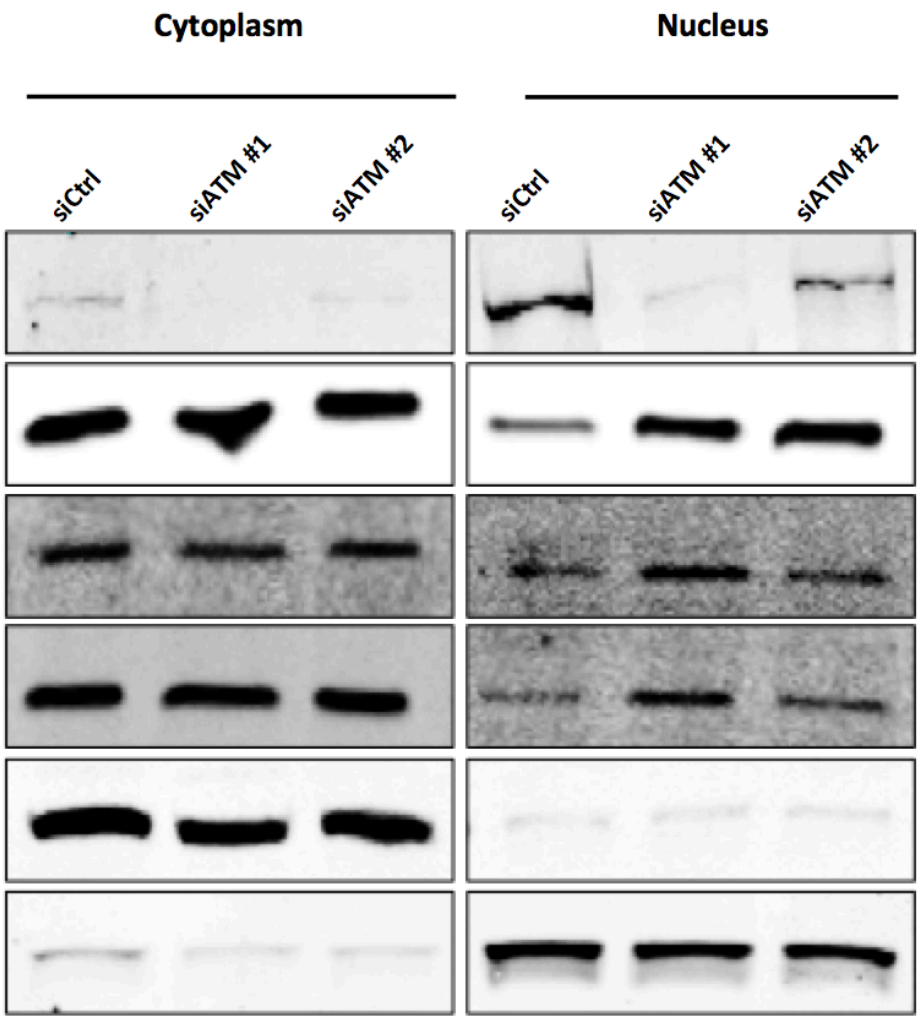


Fig.7 Proteomics data showing the fold of change in proteasome subunit in cell extracts from ATM-depleted cells. Data are displayed as in **Fig. 3**.



PMSD13:	1.00±0.04	1.32±0.06	1.2±0.01	1.00±0.01	3.0±0.05	2.4±0.04
PMSB5:	1.00±0.05	1.24±0.03	1.41±0.01	1.00±0.01	2.9±0.07	1.7±0.01
PMSA5:	1.00±0.02	1.21±0.03	1.33±0.03	1.00±0.04	2.4±0.03	1.6±0.05

Fig.8 Representative Western blot picture validating the SILAC proteomics data. TIG-1 fibroblasts were transfected with two different ATM-targeting siRNAs (siATM #1 or siATM #2) for seventy-two hours. Hsp90 and Ku80 were used as a loading control for the cytoplasmic and nuclear compartment, respectively. 25 µg of protein were loaded on a 16% polyacrylamide gel. Densitometric quantification of each subunit (with the mean ± SD from three independent experiments) is reported at the bottom.

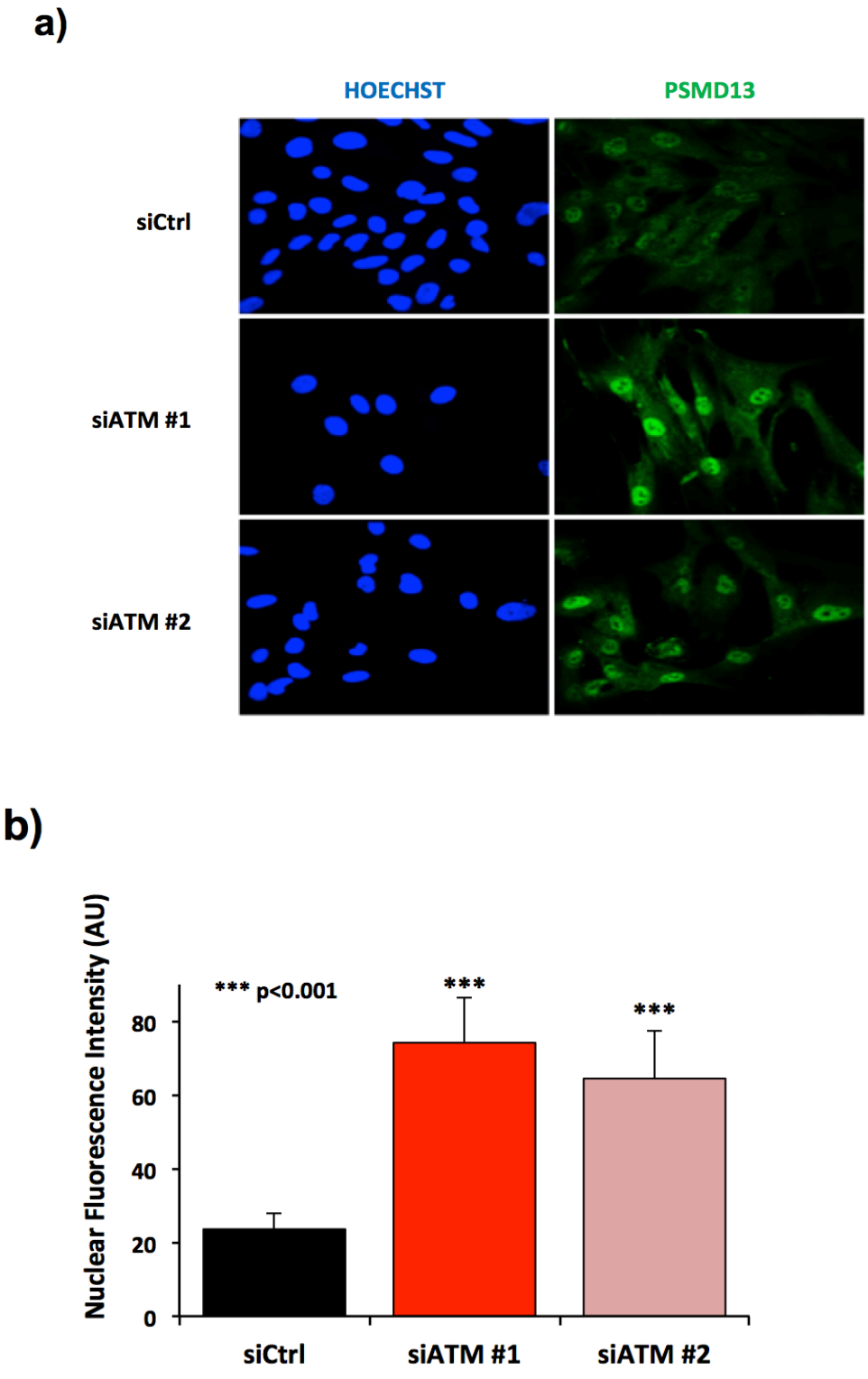


Fig.9 a) Representative immuno-fluorescence micrographs validating the SILAC proteomics data. Seventy-two hours after transfection with ATM-targeting siRNAs the level of PSMD13 was analysed by immunofluorescence. Hoechst 33342 was used to stain nuclei. **b)** Histograms showing quantification of nuclear PSMD13 intensity from at least 15 cells in **a)**. (*** p<0.001).

2.2.2 Nuclear proteasome subunits in ATM-depleted fibroblasts are fully active

Effective proteolysis does not only require accumulation of proteasomal particles in the nucleus: these particles must be in their catalytically competent form. We asked whether an upregulation in the amount of proteasome subunits in the nuclear compartment could be accompanied by an increased nuclear proteolytic activity. The chymotrypsin-like proteasomal activity in ATM-depleted cell extracts was measured using a fluorimetric assay (see “Materials and methods” for details). Consistent with our hypothesis, we confirmed that the proteasome activity was significantly increased in the nuclear, but not in the cytoplasmic compartment of ATM-depleted cells (Fig. 10). Indeed, seventy-two hours after ATM knockdown nuclear proteolytic activity rose by 1.75 fold in cells transfected with siATM #1 and 1.5 fold in cells transfected with siATM #2, whereas cytoplasmic proteolytic activity was not significantly changed in any of the samples (Fig. 10). The results of the assay are entirely consistent with the proteomics data shown in Fig. 7 and with our observations using Western blot (Fig. 8) and immunofluorescence (Fig. 9). Moreover, these data demonstrate that the fraction of the proteasome in the nucleus of ATM-depleted cells is functionally competent.

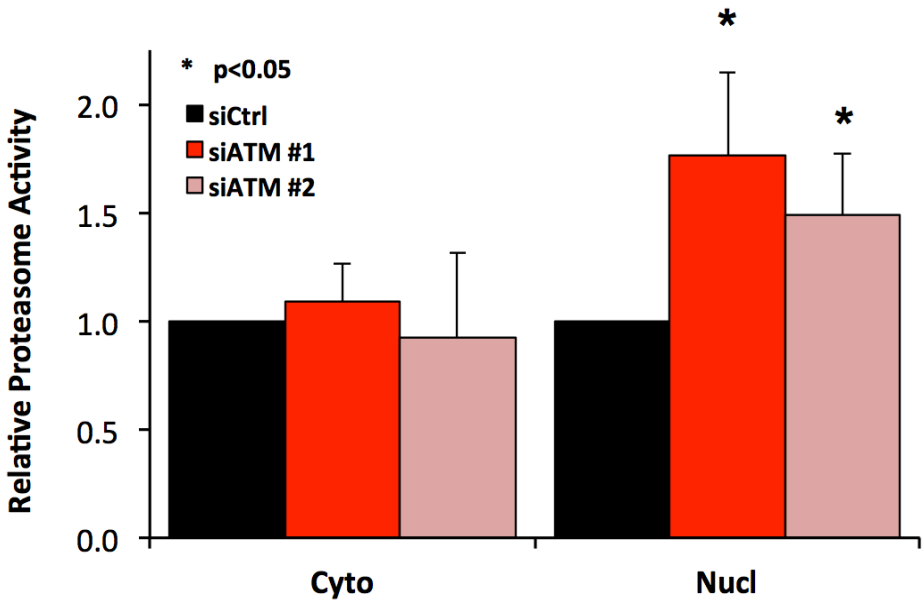


Fig.10 Histogram showing the quantification of chymotrypsin-like activity in cells depleted of ATM. Elevated proteolytic activity was detected in the nuclear compartment of ATM-depleted fibroblasts. 1 µg of cytoplasmic protein extract or 5 µg of nuclear protein extract was incubated with 50 µM Suc-LLVY-AMC; fluorimetric intensity of the cleaved substrate was measured as described in Materials and Methods. Data obtained from ATM-depleted cells was normalised to siCtrl cells. The histogram expresses the mean ± SD from three independent experiments (* p<0.05).

2.3 ATM-depleted cells modulate proteolysis to counteract oxidative stress in the nucleus

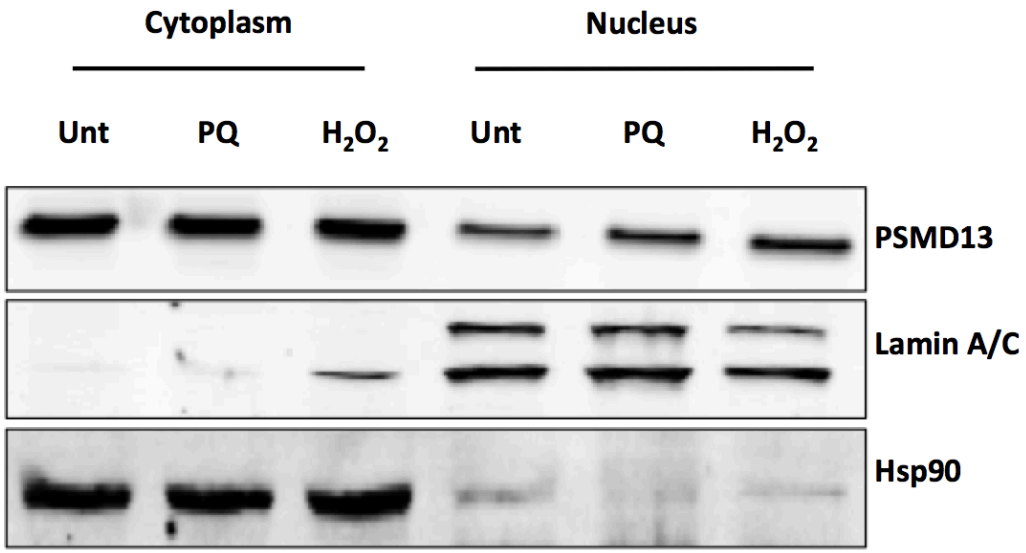
2.3.1 Oxidative stress affects localisation of the proteasome

Our observations suggest that ATM-depleted fibroblasts progressively accumulate oxidative stress and promote proteasome localisation in the nuclear compartment. We postulated that the upregulation of nuclear proteolysis could contribute to the turnover of oxidised proteins. To confirm this, we assessed whether similar rearrangement of the proteolytic machinery could be observed under conditions of oxidative stress.

We analysed the response of normal fibroblasts to two ROS-generating agents, namely paraquat (PQ) and H_2O_2. PQ is a widely used insecticide that is processed by mitochondria and converted into PQ-radical. PQ-radical reacts rapidly with oxygen, generating superoxide and peroxide radicals (Bus & Gibson, 1984). In order to mimic the situation of prolonged ROS increase observed during ATM depletion, we subjected cells to a persistent treatment (72 hours), providing fresh oxidative agents every 24 hours. Western blot data highlighted an increase in the nuclear amount of PSMD13 in PQ- and H_2O_2-treated cells (Fig. 11), which was similar to what we observed in ATM-depleted cells (Fig. 8). Moreover, the level of carbonylated proteins in PQ- and H_2O_2-treated cells increased substantially in the nuclear compartment (Fig. 12). We concluded that cells exposed to persistent oxidative stress modulate their proteolytic capacity in the nuclear compartment, likely to prevent accumulation of toxic oxidised species.

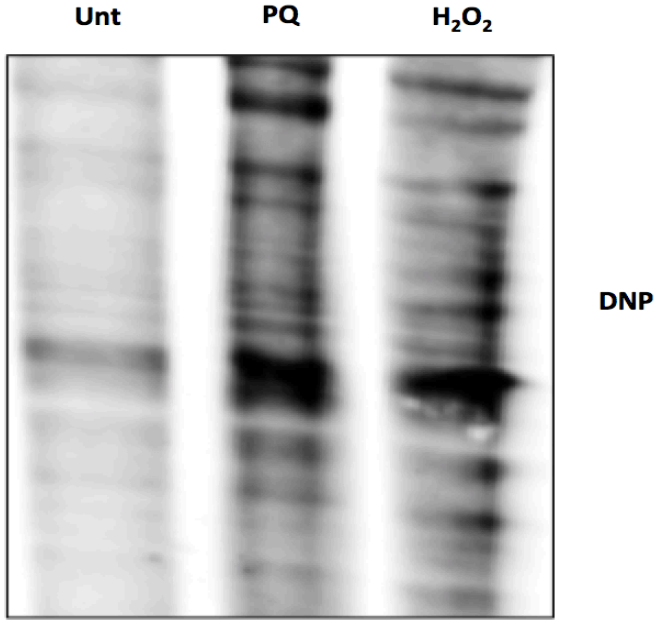
In order to further evidence that elevated nuclear proteolysis correlates with the accumulation of oxidatively damaged proteins, we treated ATM-depleted fibroblasts with a proteasome inhibitor (MG132). The amount of carbonylated proteins was subsequently analysed by Western blot. As illustrated in Fig. 13, a high amount of nuclear carbonylated proteins was induced by ATM depletion. Remarkably, an even greater level of protein carbonylation could be observed when proteasome activity was inhibited by MG132. Cells treated with H_2O_2 were used as a positive control; the content of carbonylated proteins also increased dramatically when H_2O_2 was used together with the proteasome inhibitor.

Altogether, our data support the hypothesis that induction of cellular oxidative stress upon loss of ATM is counteracted by modulation of cellular proteolysis, in particular by increasing the amount of functional 26S proteasome in nucleus.



PSMD13: **1.03±0.01** **0.98±0.04** **1.01±0.02** **1.00±0.02** **1.62±0.08** **2.5±0.05**

Fig.11 Western blot analysis showing that PQ- and H_2O_2-treated cells exhibit increased amount of the proteasome subunit PSMD13 in the nuclear fraction. TIG-1 fibroblasts were treated with either 150 μM H_2O_2 or 125 μM PQ and harvested after 72 hours. Drugs were fed fresh every 24 hours. Hsp90 and lamin A/C were used as loading controls for the cytoplasmic and nuclear fractions, respectively. 25 μg of cell extracts were loaded on a 16% polyacrylamide gel. Densitometric quantification of PMSD13 (with the mean ± SD from three independent experiments) is reported at the bottom.



DNP: **1.00±0.03** **1.6±0.03** **1.5±0.02**

Fig.12 Analysis of nuclear oxidised proteins in PQ- and H2O2- treated cells. TIG-1 fibroblasts were treated as in **Fig. 11**. Oxidised proteins were derivatised with DNP and blotted with an antibody against DNP as described in "Materials and Methods". 10 μg of nuclear cell extracts were loaded on an 8% polyacrylamide gel. Quantification of the DNP signal (with the mean ± SD from three independent experiments) is reported at the bottom.

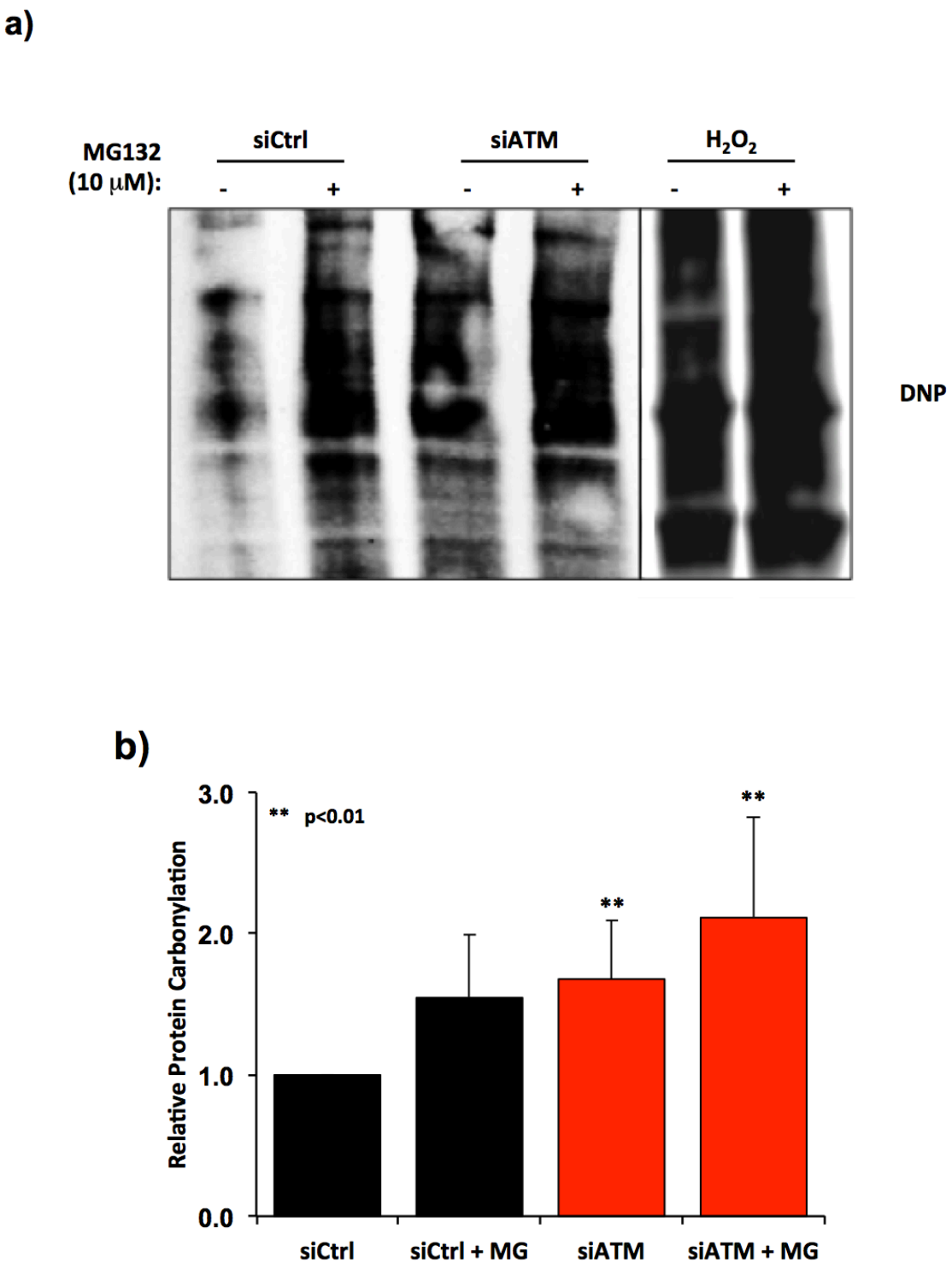


Fig.13 a) Representative Western blot showing increased accumulation of nuclear oxidised proteins in ATM-depleted cells treated with the proteasome inhibitor MG132. Cells transfected with either siCtrl or siATM were incubated with 10μM MG132 (6 hours). Cells treated with 1mM H2O2 for 30 minutes were used as a positive control. 10 μg of nuclear cell extracts were loaded on an 8% polyacrylamide gel. **b)** Histograms showing quantification of protein carbonylation in **a)**. (** p<0.01).

2.3.2 Proteolysis is important for survival of ATM-depleted fibroblast

Our data show that ATM-depleted fibroblasts experience proteostatic stress due to accumulation of oxidative protein damage. This situation is dealt with by rearranging the proteasome and increasing proteolysis in the nuclear compartment. These observations suggest that survival of cells lacking ATM could rely on active proteolysis. To assess the possibility, we measured the sensitivity of ATM-depleted cells to the proteasome inhibitors MG132 and bortezomib. Bortezomib is a peptide boronate proteasome inhibitor that acts more potently than MG132 (Bonvini et al., 2007). Cell viability experiments showed that lack of ATM sensitises cells to both proteasome inhibitors (Fig. 14). As illustrated by the histogram, 24h after treatment with the inhibitors viability of ATM-depleted cells dropped by 50% (MG132) and 60% (bortezomib) respectively. The decrease in cell viability was significantly greater than that of control cells (12% for MG132 and 33% for bortezomib).

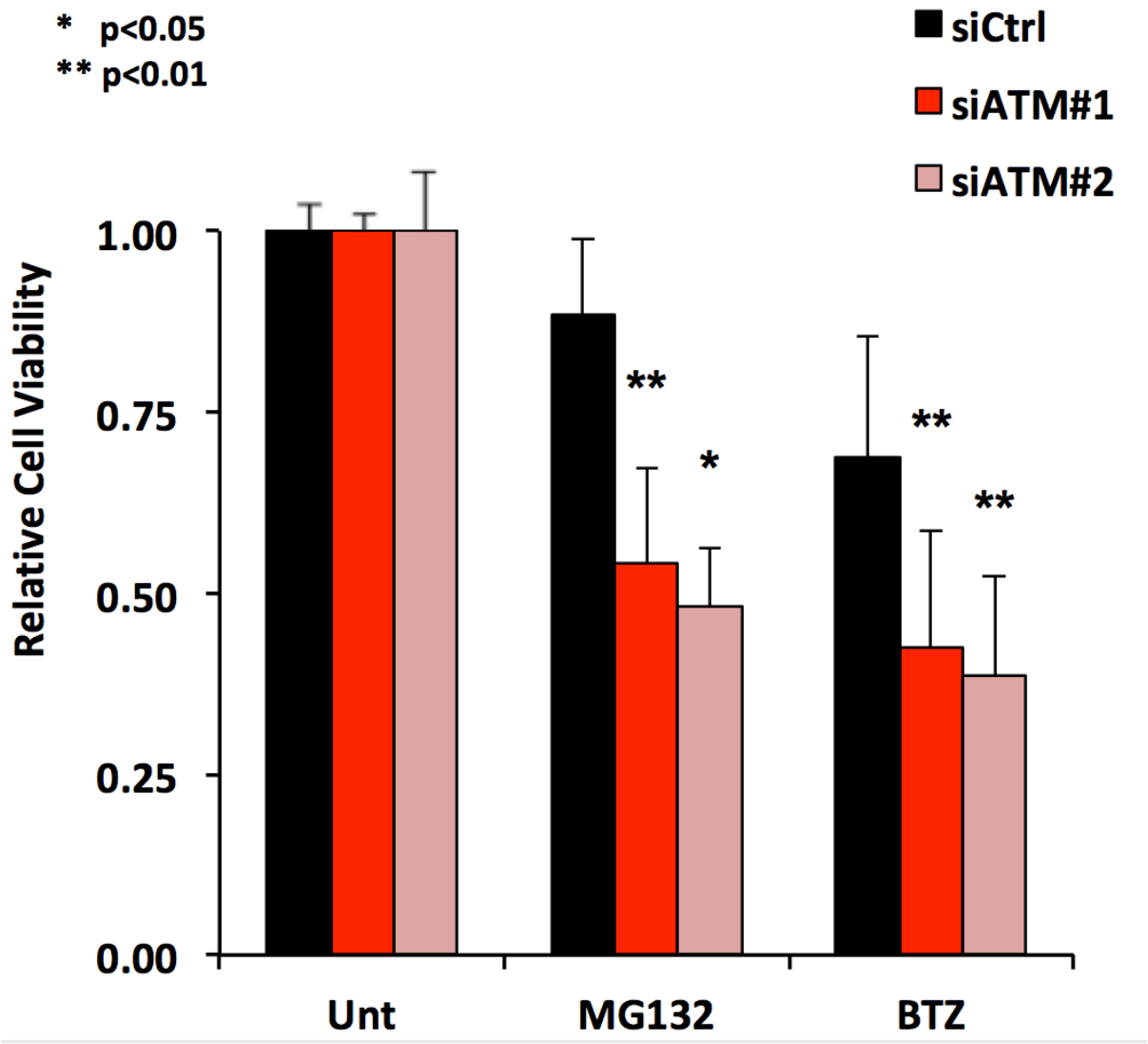


Fig.14 Viability assay showing that ATM depletion sensitises cells to proteasome inhibitors. Cells were incubated with either 500 nM MG132 or 50 nM bortezomib (BTZ) for 24 hours. The number of surviving cells was scored using Trypan blue staining. The histogram displays the mean ± SD obtained from three independent experiments (* p<0.05, ** p<0.01). Unt: DMSO-treated cells.

While this could indicate that ATM-depleted fibroblasts are hypersensitive to proteasome inhibition, ATM has been shown to modulate a variety of ubiquitylation/deubiquitylation-dependent signalling pathways. For example, during the DDR, recruitment of p53-binding protein 1 (53BP1) and breast cancer type 1 susceptibility protein (BRCA1) to damage sites is promoted through ATM-dependent ubiquitination of histone H2A by RNF168, which is important for optimal DSB repair via non-homologous end-joining (NHEJ) and homologous-recombinant repair (HRR) (Brown & Jackson, 2015).

Moreover, ATM-dependent ubiquitination of histone H2B by RNF20 has been shown to regulate chromatin condensation; playing an important role for optimal DSB repair (Moyal et al., 2011) (Nakamura et al., 2011). As inhibition of proteolytic activity interferes with the dynamics of intracellular ubiquitin pool (Kaiser et al., 2011), inhibition of the proteasome may affect cell viability via an impaired DDR, rather that excessive accumulation of oxidised protein species. In order to take into account any effects played by ATM- and ubiquitin-dependent pathways on cell sensitivity to proteasome inhibition, we measured cell survival upon depletion of either RNF20 or 53BP1. Importantly, while ATM depletion impacted cell survival in the presence of proteasome inhibitors, depletion of RNF20 and 53BP1 alone did not affect sensitivity to MG132 (Fig. 15). Our results do not exclude that ATM depletion may lead to perturbation of the ubiquitin pools. However, our data suggest that in the absence of ATM, disruption of cellular ubiquitylation pool or DNA repair *per se* are not major factors affecting cell sensitivity to proteasome inhibition.

Altogether, these results strongly suggest that proteolytic activity is required for survival of ATM-depleted cells at the early stages after ATM loss.

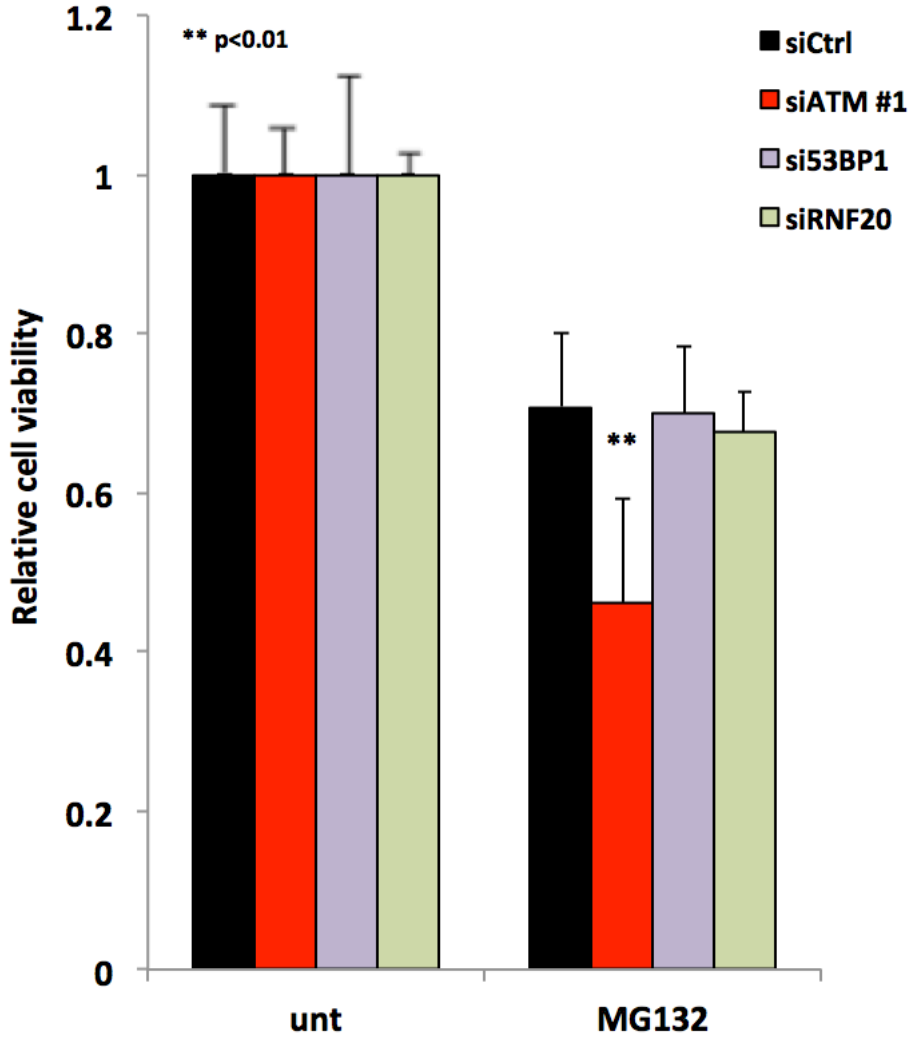
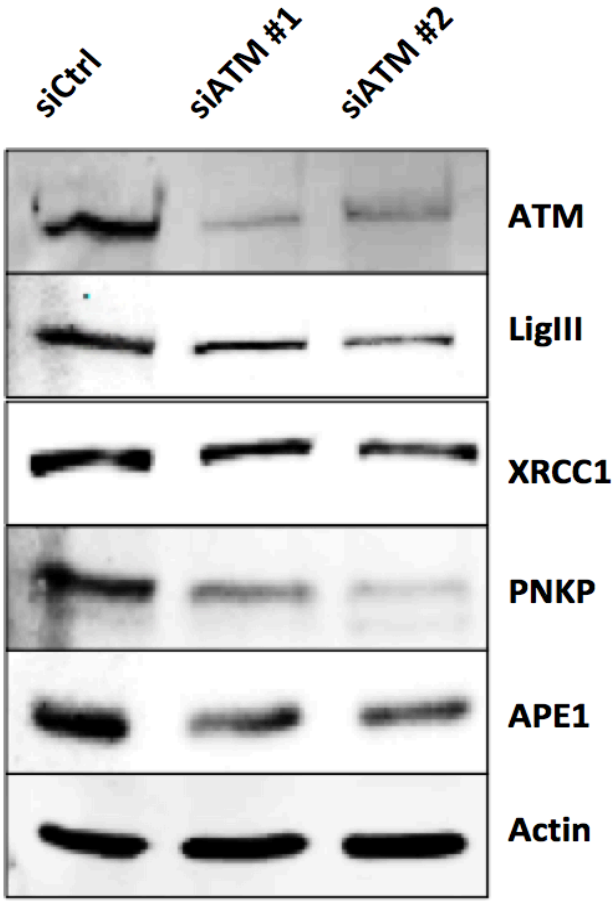


Fig.15. Histogram showing that loss of RNF20- and 53BP1- mediated signalling pathways does not sensitise cells to proteasome inhibition. The experiment was carried out as in **Fig. 14**, using the indicated siRNA (** p<0.01).

2.4 Impaired BER capacity and genomic instability in ATM-depleted cells

2.4.1 BER components are downregulated in ATM-depleted cells

Together with proteins, DNA is also susceptible to oxidative stress (Avery, 2011) (Schieber & Chandel, 2014). Products of oxidative DNA damage are normally eliminated by BER. The BER pathway is a fundamental DNA repair system acting both on mitochondrial and nuclear DNA, and the main localisation of BER component is thought to be the cellular nucleus (Dianov & Hübscher, 2013). The existence of a cross-talk between ATM and BER has been discussed earlier (section 1.2). Given that ATM depletion led to increased nuclear protein turnover, we checked whether the expression of any BER factor could be affected by a lack of ATM. We observed that several components of the BER pathway including XRCC1, LigIII, PNKP and APE1 were downregulated at the protein level in cells deficient for ATM (Fig. 16).



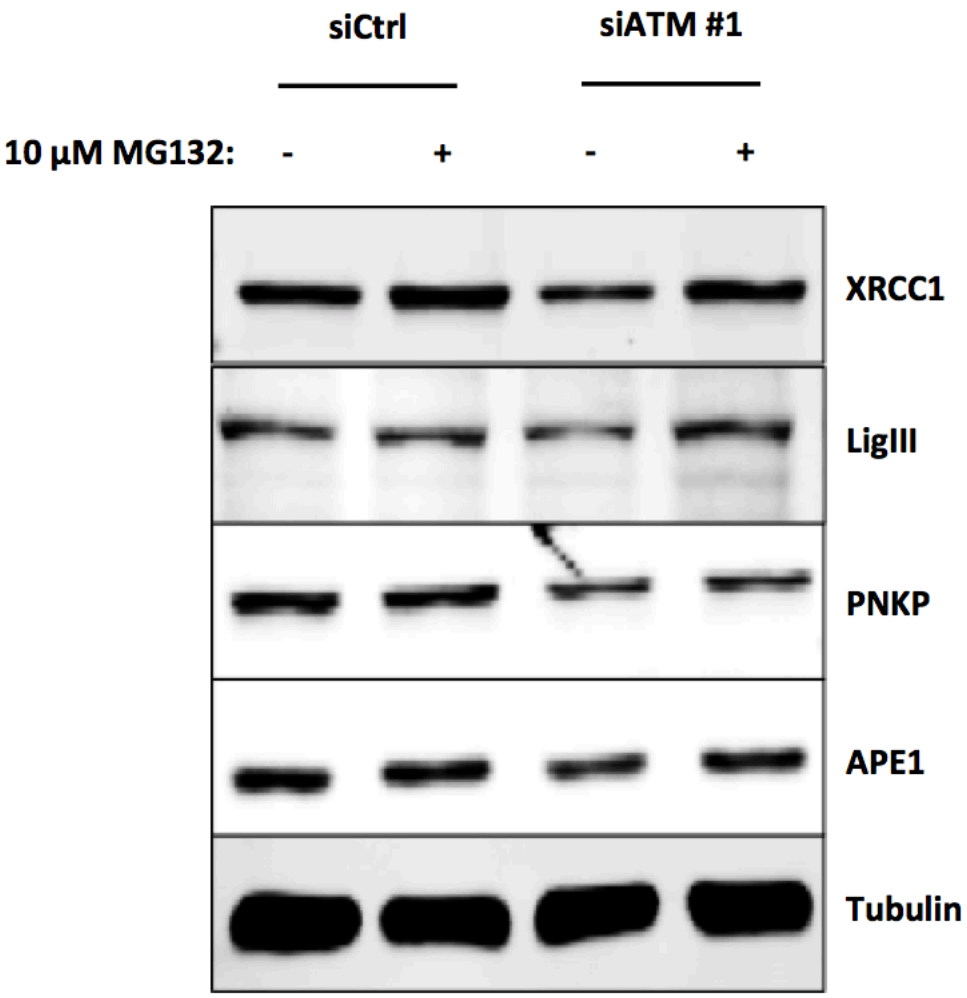
XRCC1:	**1.00±0.02**	**0.78±0.04**	**0.72±0.01**
APE1:	**1.00±0.02**	**0.70±0.01**	**0.76±0.02**
PNKP:	**1.00±0.04**	**0.72±0.03**	**0.35±0.01**
LigIII:	**1.00±0.02**	**0.80±0.01**	**0.63±0.03**

Fig.16 Representative Western blot showing downregulation of BER components in whole cell extracts from ATM-depleted fibroblasts. Actin was used as loading control. 40 µg of cell extracts were loaded on a 12% polyacrylamide gel. Densitometric quantification of the indicated proteins (with the mean ± SD from three independent experiments) is reported at the bottom.

2.4.2 Downregulation of BER components is mainly caused by elevated proteolytic activity

To assess if decreased BER expression in cells lacking ATM could be attributed to increased proteolysis, we analysed BER proteins levels in ATM-depleted cells in the presence of the proteasome inhibitor MG132. In line with our hypothesis, downregulation of BER components could

be partially rescued when proteolysis was inhibited by MG132 (Fig. 17). These data support the idea that lower BER levels in ATM-depleted cells are predominantly caused by increased proteolysis.



XRCC1:	1.00±0.04	2.13±0.03	0.64±0.01	0.93±0.05
LigIII:	1.00±0.06	1.50±0.01	0.73±0.03	1.03±0.06
PNKP:	1.00±0.04	1.14±0.02	0.35±0.02	0.72±0.02
APE1:	1.00±0.01	0.90±0.01	0.63±0.04	0.84±0.02

Fig.17 Representative Western blot showing that downregulation of BER components can be rescued by inhibition of proteolysis. Seventy-two hours after transfection with the indicated siRNA, TIG-1 cells were treated with 10 µM MG132 for additional 6 hours. 40 µg of cell extracts were loaded on a 12% polyacrylamide gel. Densitometric quantification of the indicated proteins (with the mean ± SD from three independent experiments) is reported at the bottom.

2.4.3 BER capacity is impaired in ATM-depleted cells

Downregulation of DNA repair proteins can lead to deficiency in DNA repair capacity (Markkanen et al., 2015) (Poletto et al., 2016). As expression of BER proteins was dramatically affected by loss of ATM, we hypothesised that this could have a negative effect on the BER capacity of ATM-depleted cells. To check this, we performed a set of *in vitro* assays where cell extracts obtained from ATM-depleted cells were incubated with oligonucleotides containing different lesions. This allowed us to evaluate the efficiency of individual steps of the BER pathway. Fig. 18 and 19 demonstrate the results of two different *in vitro* assays: the AP site incision and nick ligation assays (see "Materials and methods" for specific details on the assays). The AP site incision assay assesses the efficiency of AP site endonucleolytic cleavage by APE1 in a whole cell extract. Our data indicate that total AP-endonuclease activity was impaired following loss of ATM (Fig. 18). This was entirely consistent with the lower amount of APE1 measured upon ATM depletion (Fig. 16). We also evaluated the ligation efficiency of a DNA substrate bearing a SSB. In mammalian cells, DNA ligation is mainly carried out by DNA LigIII and LigI; LigIII is generally found in a protein complex containing XRCC1, which promotes DNA ligation involved in short-patch BER (Caldecott et al., 1994) (Cappelli et al., 1997). In line with the lower LigIII and XRCC1 content in ATM-depleted fibroblasts (Fig 16), nick ligation activity was also remarkably decreased in nuclear extracts obtained from ATM-depleted cells (Fig 19). Notably, when we mimicked the decline in BER components observed in ATM-depleted fibroblasts by using a partial depletion approach, we observed a similar impairment in both AP site incision (Fig 20) and nick ligation (Fig 21) activity. We did not observe additional impairment in BER capacity when ATM was depleted simultaneously with either APE1 or LigIII (Fig. 20 and 21).

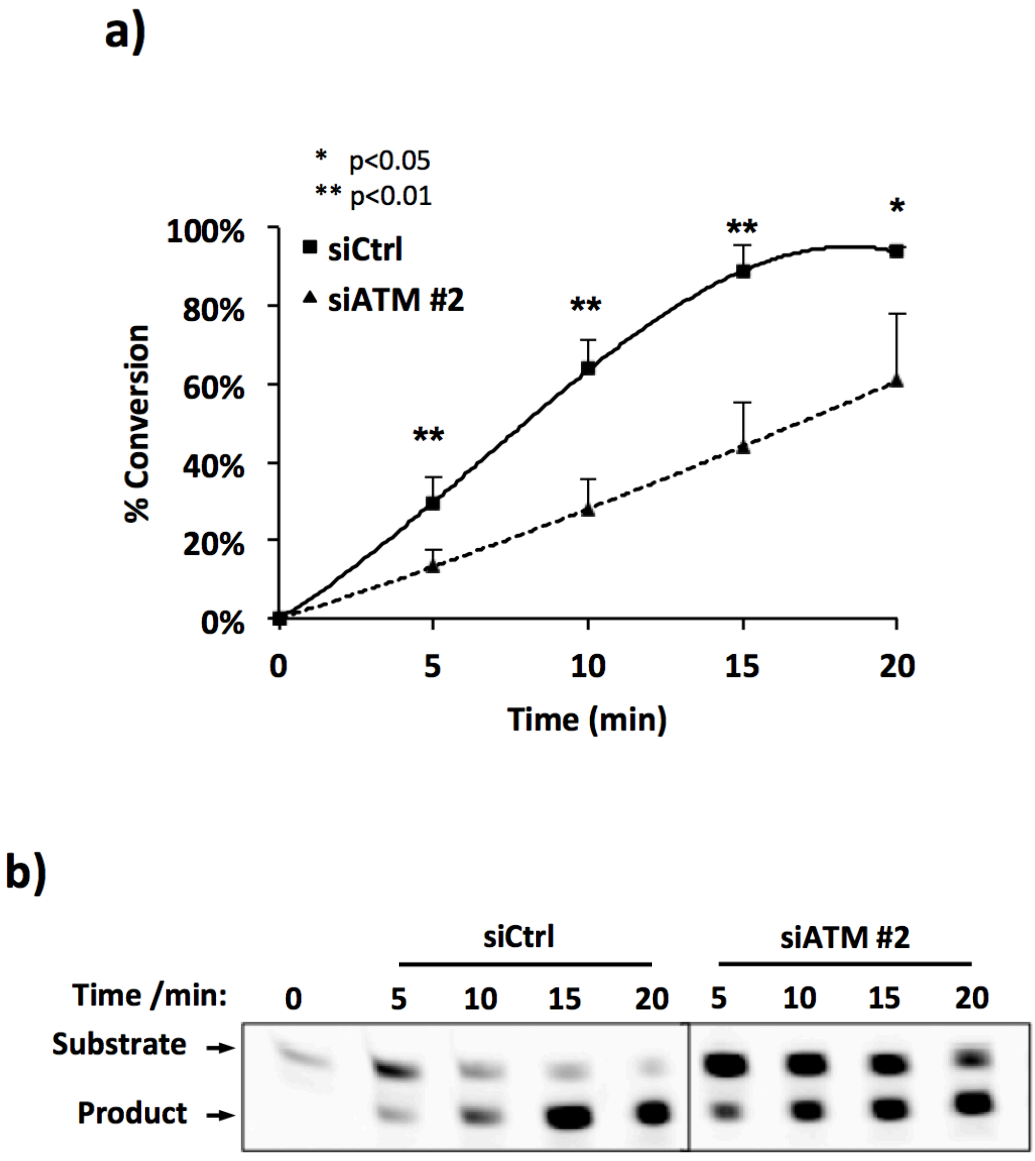


Fig.18 AP site incision assay revealing deficiency in AP-endonuclease activity in ATM-depleted cells. **a)** Whole cell extracts obtained from either siCtrl-treated cells or siATM-treated cells were assessed for their ability to cleave a DNA substrate containing an AP site. The curve represents the conversion rate of an oligonucleotide substrate to its cleaved product versus reaction time from three experimental replicates (* $p<0.05$, ** $p<0.01$). **b)** A representative scan of a time course showing lower substrate to product conversion in ATM depleted cells.

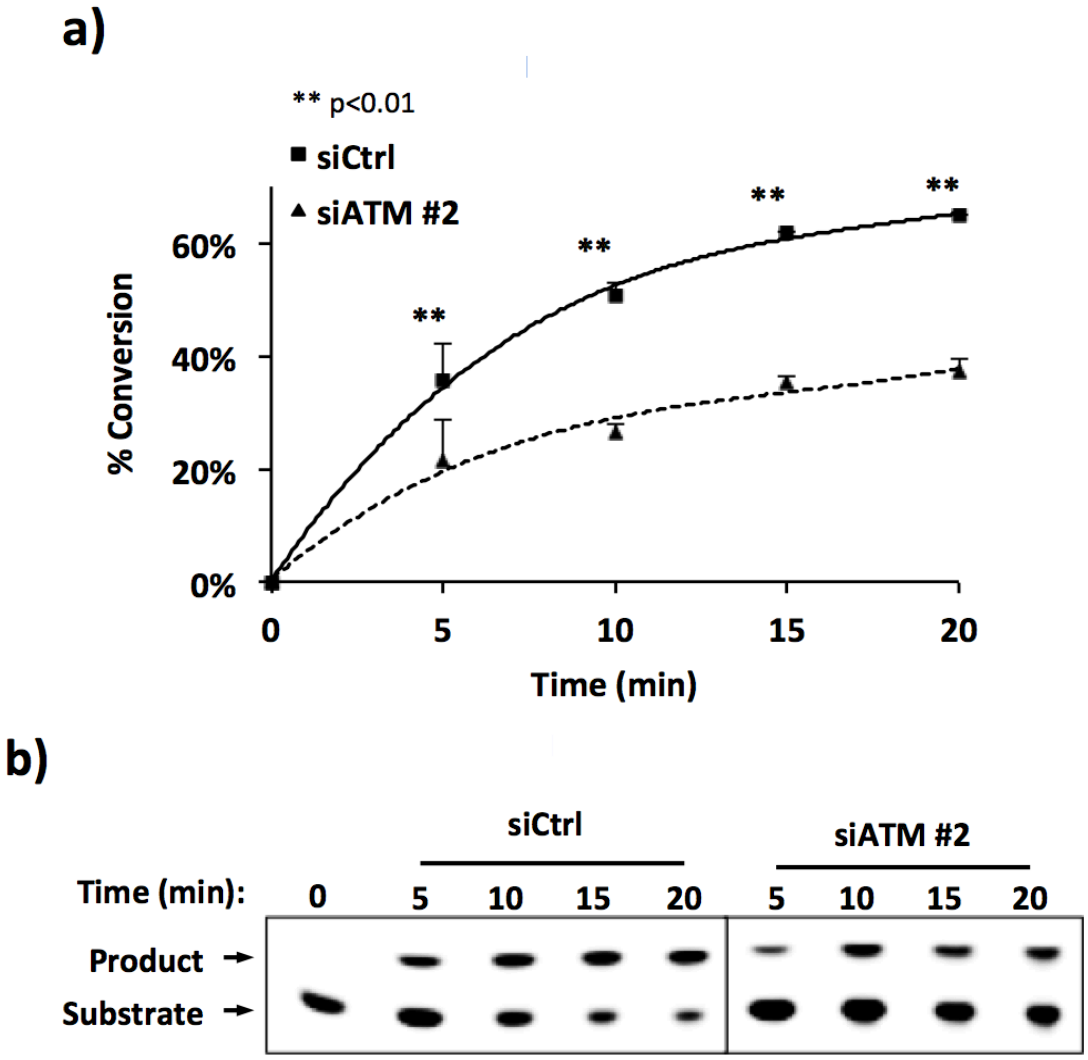
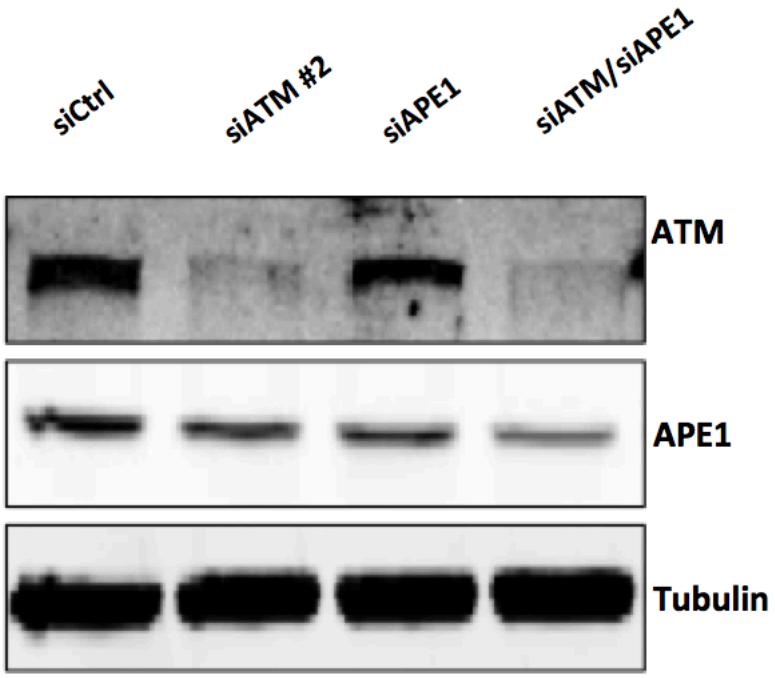


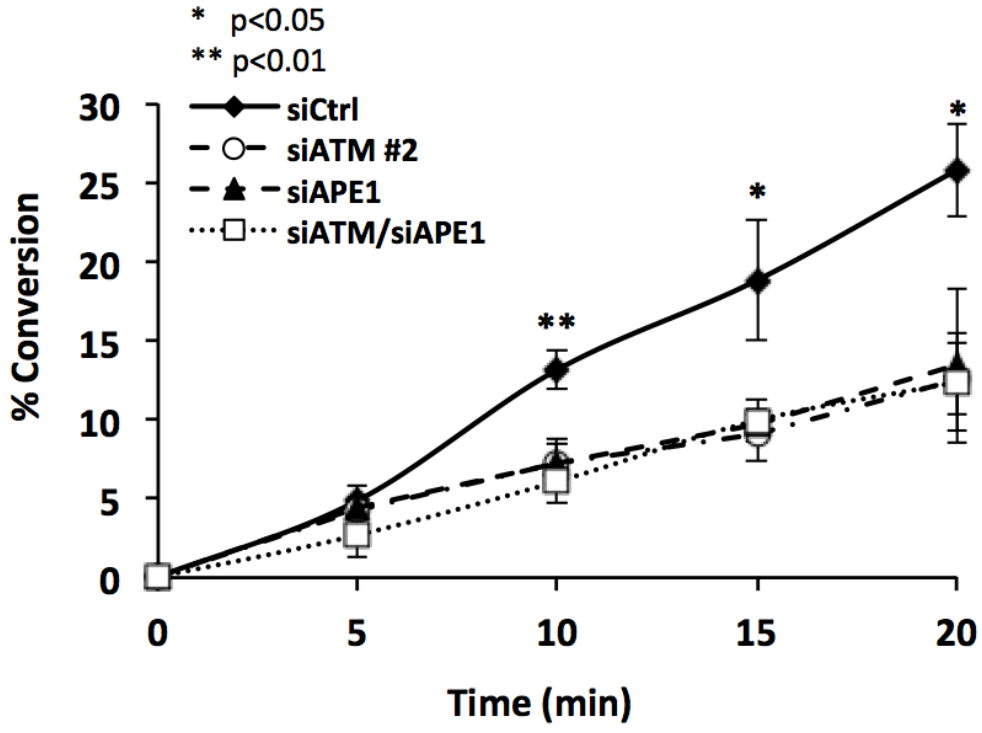
Fig.19 Nick-ligation assay revealing impaired nick ligation activity 3 in ATM-depleted cells. Nuclear cell extracts obtained from either siCtrl-treated cells or siATM-treated cells were assessed for their ability to ligate a DNA substrate containing a SSB. The curve represents the conversion rate of an oligonucleotide substrate to its ligated product versus reaction time from three experimental replicates (** p<0.01). **b)** A representative scan of a time course showing lower substrate to product conversion in ATM depleted cells.

a)



APE1: 1.00±0.03 0.82±0.03 0.81±0.01 0.61±0.02

b)

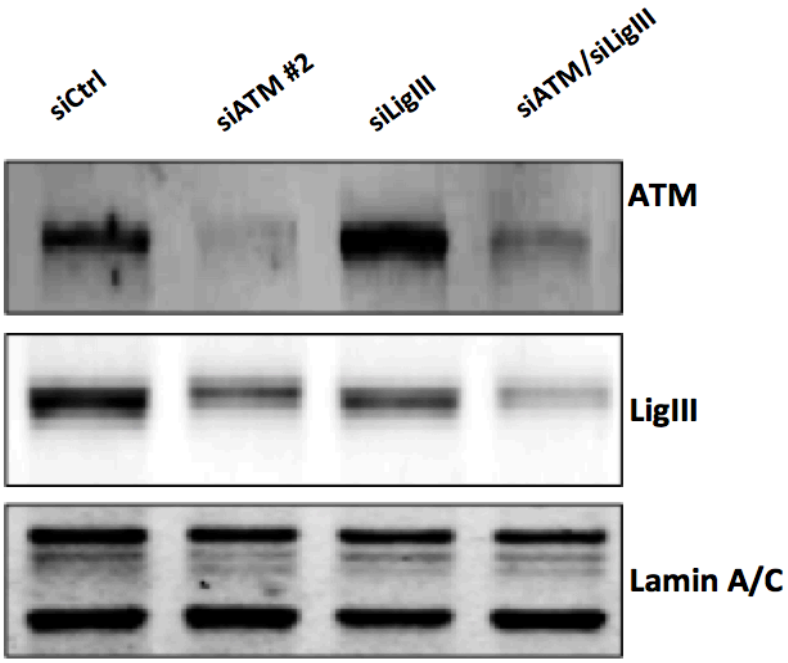


c)



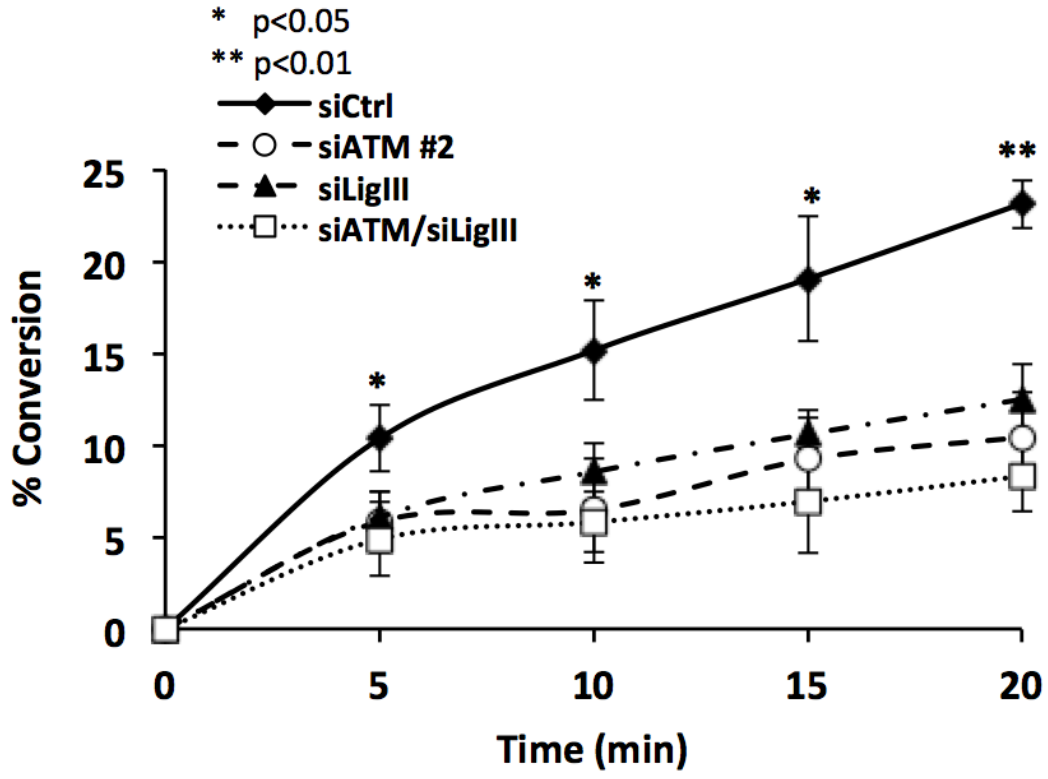
Fig.20 AP site incision assay in ATM- and APE1-depleted cells. To achieve a mild APE1 depletion, TIG-1 cells were transfected as indicated in "Materials and methods". **a)** Western blot analysis assessing APE1 and ATM depletion. Quantification of the indicated proteins (with the mean ± SD from three independent experiments) is reported at the bottom. **b)** Conversion rate of substrate to product versus reaction time. **c)** A representative scan showing the conversion rate of the substrate to the product in the assay. (* $p<0.05$, ** $p<0.01$)

a)



LigIII: 1.00±0.01 0.64±0.02 0.73±0.06 0.51±0.02

b)



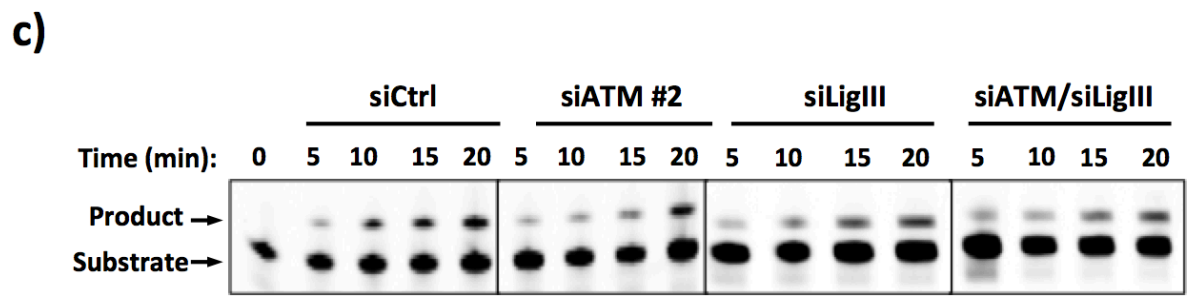


Fig.21 Nick-ligation assay in ATM- and LigIII-depleted cells. Data are presented as in **Fig. 20**. To achieve a mild LigIII depletion, TIG-1 cells were transfected as indicated in "Materials and methods". **a)** Western blot analysis assessing LigIII and ATM depletion. Quantification of the indicated proteins (with the mean ± SD from three independent experiments) is reported at the bottom. **b)** Conversion rate of substrate to product versus reaction time. **c)** A representative scan showing the conversion rate of the substrate to the product in the assay. (* $p<0.05$, ** $p<0.01$)

To further back up our observations, we carried out *in vivo* DNA repair assays in cells treated with two different BER eliciting agents: the alkylating compound methyl methanesulfonate (MMS) and the oxidative agent H_2O_2. After treating cells with either MMS or H_2O_2, the progression of DNA repair was quantified throughout a recovery period using the alkaline comet assay. While control cells showed efficient repair rates, we observed remarkable repair impairment in ATM-depleted cells in response to both genotoxins (Fig. 22). This was consistent with the downregulation of BER components measured upon loss of ATM (Fig. 16) and with impairment on both AP endonuclease (Fig. 18) and nick-ligation activity (Fig. 19) observed in ATM-depleted fibroblasts.

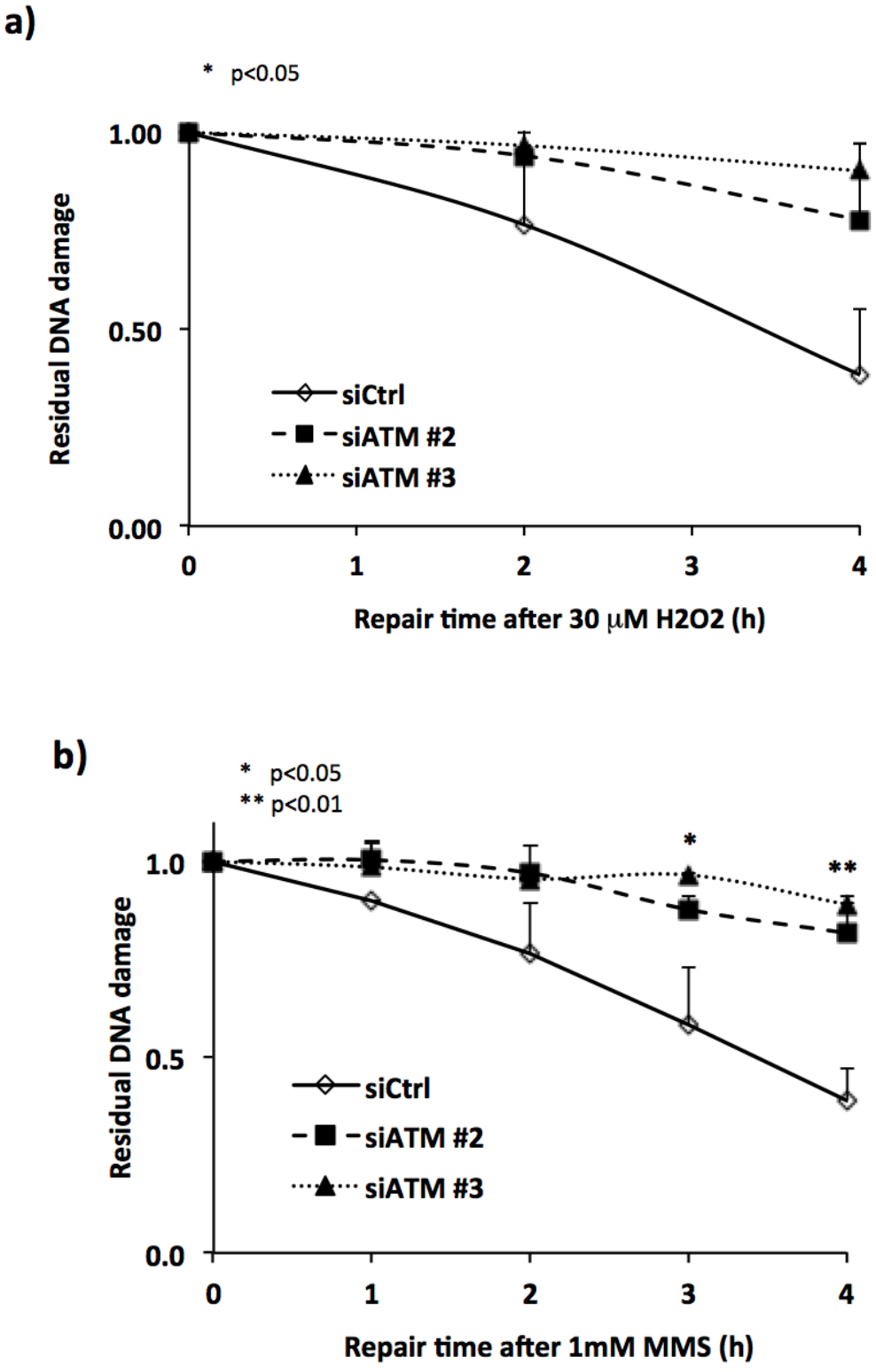
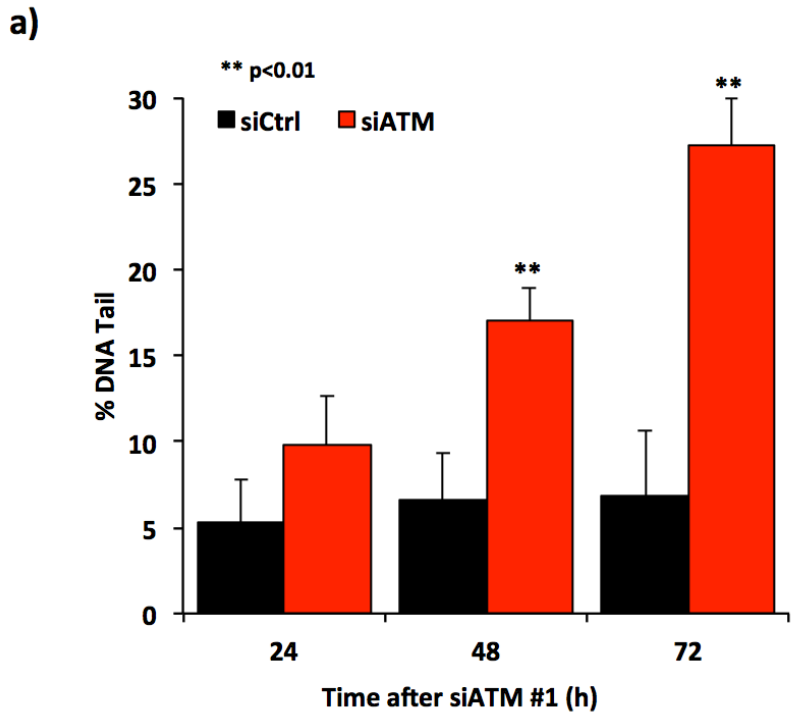


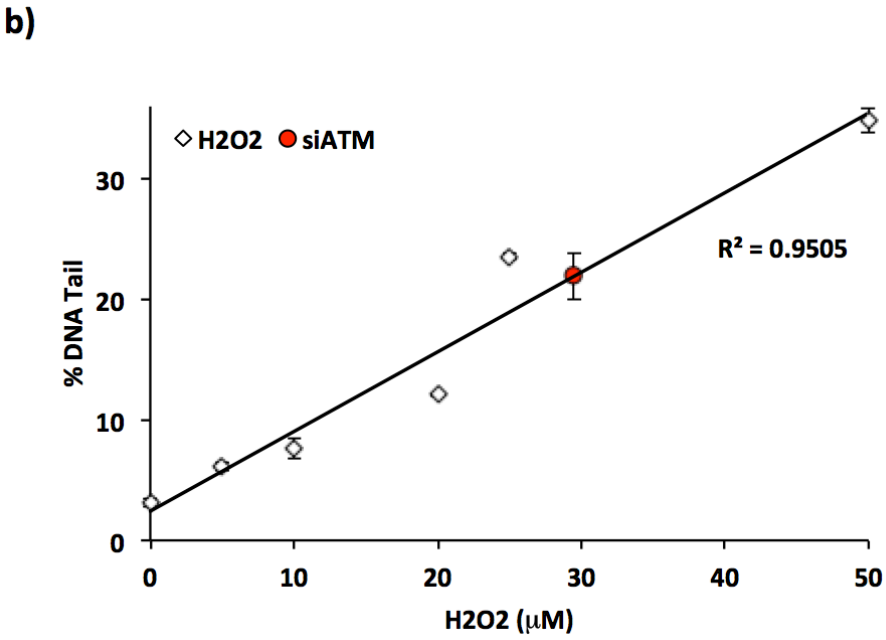
Fig.22 Slower DNA repair kinetics in ATM-depleted cells, as measured using the alkaline comet assay. The curves represent the relative amount of DNA damage remaining after recovering from **a)** H_2O_2 and **b)** MMS treatment. Cells transfected with the indicated siRNA were treated with either of the reagents at the indicated concentration for 10 minutes, followed by repair at 37°C for 0-4 hours.

2.4.4 ATM-depleted fibroblasts accumulate DNA strand breaks at early stages after ATM loss

While SSBs originate spontaneously at a very high rate (Lindahl et al., 1993 Nature) – especially in a condition of impaired BER – DSBs mainly originate during the S phase of the cell cycle due to collapse of the replication fork at SSBs (Caldecott, 2008). DSBs are one of the main threats to genome integrity, as they can result in chromosomal aberrations (Gent et al., 2001); therefore accumulation of DSBs is conventionally regarded as a biomarker of genomic instability and genotoxicity. Since the BER pathway and DNA repair capacity are significantly impacted by ATM loss, we asked whether spontaneous DNA damage might accumulate in fibroblasts at early stages upon ATM depletion. DNA damage was measured over a time-course after ATM depletion using both the alkaline and the neutral comet assay. These assays differ slightly in the kind of DNA damage detected. In the alkaline comet assay DNA is allowed to unwind under alkaline conditions (pH > 13). Therefore, this assay detects a variety of alkali-labile DNA lesions, including SSBs and DSBs, as well as AP sites (Collins et al., 2008). Conversely, the neutral comet assay detects mainly DNA DSBs under neutral pH conditions. By analysing the intensity of comet tails obtained using the alkaline comet assay, we found that ATM depletion led to progressive accumulation of spontaneous DNA damage as early as 48 hours after transfection (Fig. 23a). To appreciate the magnitude of the DNA damage generated upon loss of ATM, we compared these comet assays with a titration curve obtained with H_2O_2 (0 to 50 µM). Using the dose-response curve, we estimated that the amount of DNA damage induced in ATM-depleted cells 72 hours post-transfection was comparable to that produced by 30 µM H_2O_2 (Fig. 23b). Notably, the amount of lesions generated by ATM knockdown is perfectly consistent with the estimated amount of ROS that accumulate upon ATM depletion (compare Fig. 23b and Fig. 5). To characterise more specifically the type of DNA lesions induced upon ATM depletion, we also performed neutral comet assays on the same time-course shown in Fig. 23a. We observed that cells depleted for ATM also exhibited a time-dependent accumulation of DSBs Fig 23c, which is in agreement with the damage pattern obtained using the alkaline comet assay. Taken together, these

data suggest that as early as 48h after loss of ATM, normal human fibroblasts begin to accumulate spontaneously generated DNA lesions in the form of both SSBs and DSBs.





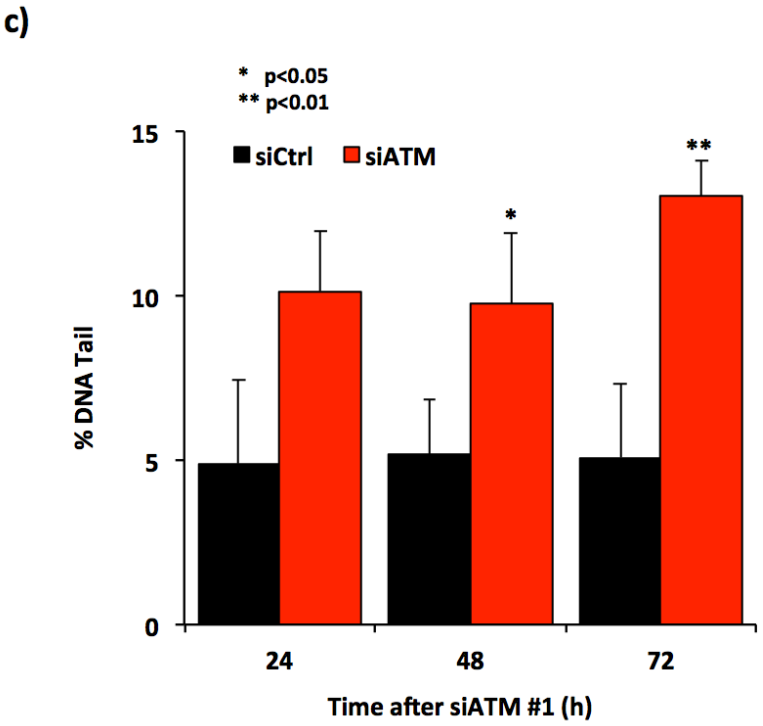


Fig.23 Comet assays showing that different types of DNA lesions accumulate upon ATM depletion. **a)** Alkaline comet assay showing time-dependent accumulation of DNA strand breaks in ATM-depleted cells. **b)** Alkaline comet assay comparing the amount of DNA strand breaks generated by ATM depletion (72 hours) with DNA lesions accumulating in cells treated with H_2O_2 at the indicated concentrations. **c)** Neutral comet assay showing that DNA DSBs accumulate in a time-dependent manner upon ATM depletion. Data are reported as mean ± SD from at least three independent experiments (* $p<0.05$, ** $p<0.01$)

2.5 The adaptation mechanisms observed in transiently depleted fibroblasts persist in cells obtained from an A-T patient

2.5.1 Cells from an A-T patient exhibit high levels of oxidative stress

Our data have so far highlighted how depletion of ATM leads to accumulation of oxidative stress in normal human cells. This is counteracted by a modulation of cellular proteolysis, in particular in the nuclear compartment. On the other hand, while these mechanisms relieve proteostatic stress, increased nuclear proteolysis inevitably leads to BER impairment. This, in turn, results in a decreased

DNA repair capacity and accumulation of genomic instability, which we measure here in the form of unrepaired strand breaks.

To verify whether the phenotypes that we identified in ATM-depleted fibroblasts are meaningful in the context of A-T, we analysed fibroblasts derived from a 14-year-old individual diagnosed with A-T (AG03058) and compared them with cells obtained from a 10-year-old healthy control (GM03349). As oxidative stress is at the basis of our mechanism, we first measured the level of ROS content in A-T fibroblasts. FACS analyses confirmed that ROS levels were greater in the patient's cells (Fig. 24). We also assessed whether increased ROS resulted in the accumulation of oxidatively modified proteins. As expected, A-T cells showed significantly greater amount of oxidised proteins in the nuclear compartment (Fig. 25) suggesting that fibroblasts from A-T patients experience proteostatic stress due to accumulation of oxidised proteins.

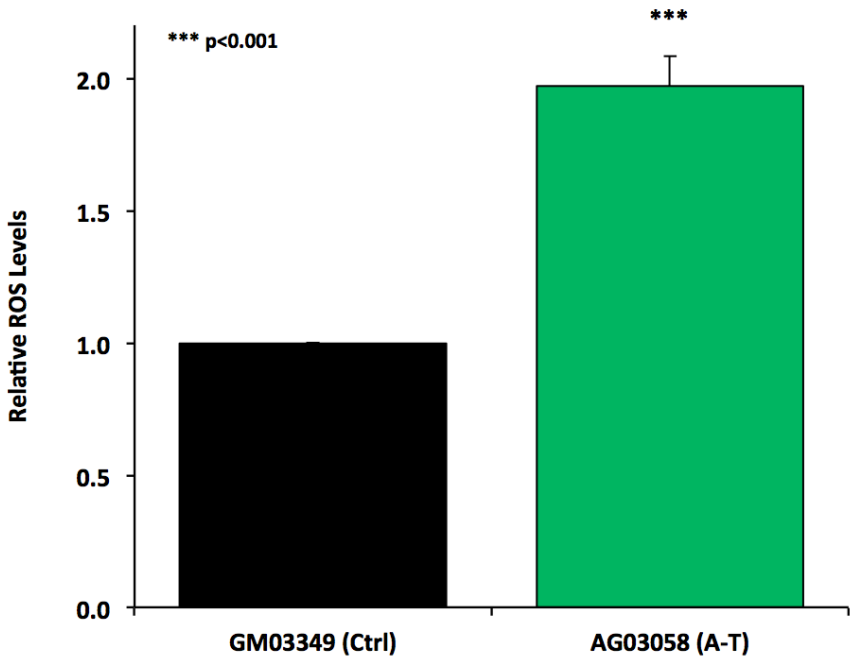


Fig.24 Flow cytometry analysis to assess ROS content in A-T cells. Histogram showing the relative amount of ROS in control and the A-T fibroblasts. The Y-axis reports the fluorescence intensity of the probe, reflecting ROS levels. The greater the fluorescence intensity, the higher the ROS content. (*** p<0.001)

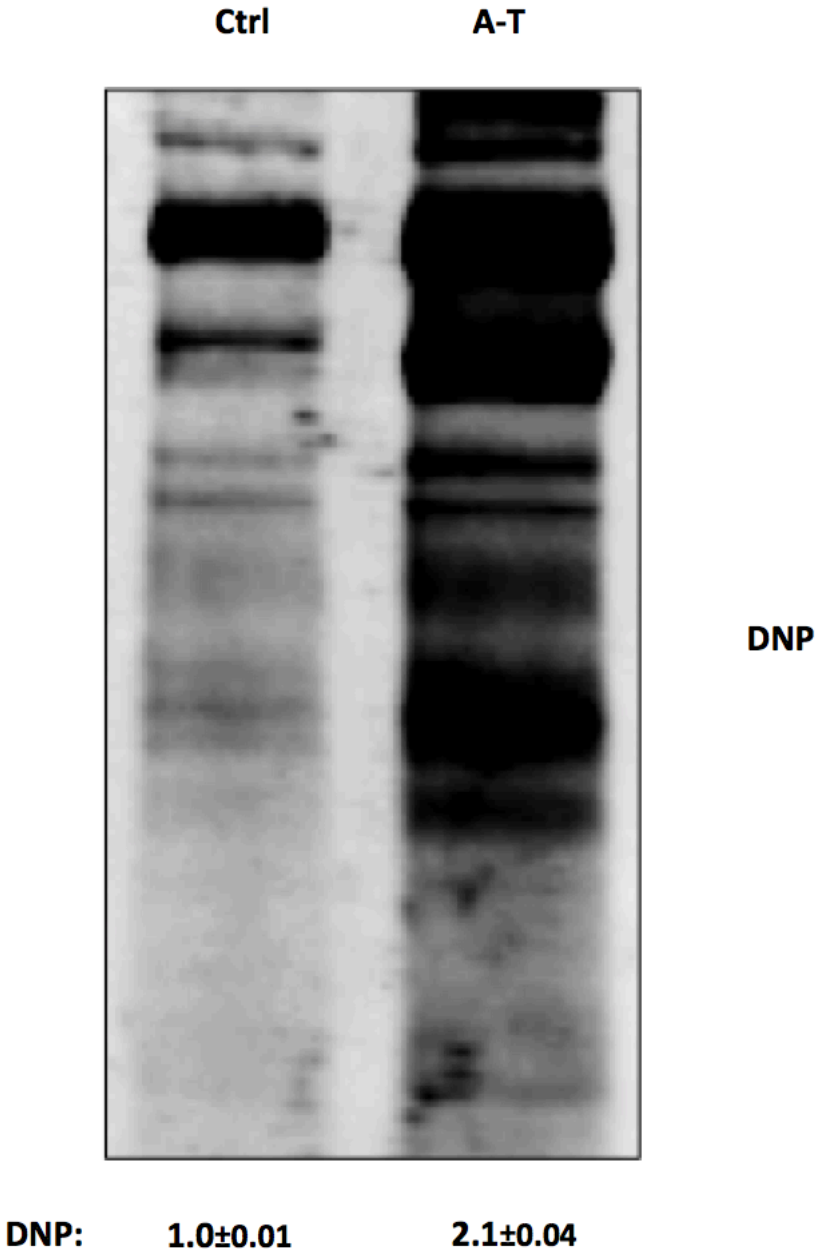


Fig.25 Representative Western blot showing increased amount of carbonylated proteins in the nuclear compartment of A-T cells. 10 µg of cell extracts were loaded on an 8% polyacrylamide gel. Densitometric quantification of DNP signal is reported at the bottom.

2.5.2 Proteolysis contributes to survival of A-T cells

Our data obtained using ATM-depleted TIG-1 cells showed that proteasome subunits were upregulated in the nuclear compartment in response to loss of ATM. Consistent with these observations, high levels of the proteasome subunit PSMD13, were detected using Western blot in

the nuclear fraction obtained from A-T cells (Fig. 26). This was also confirmed using immunofluorescence (Fig. 27), indicating that the nuclear compartment of A-T fibroblasts may also experience increased proteolysis in response to accumulation of oxidative damage.

Moreover, viability assays comparing healthy and A-T fibroblasts backed up this hypothesis (Fig. 28). After exposure to MG132, while the viability of control cells dropped by 40%, a significantly higher loss of viability was measured in A-T cells (60%). This indicates that, similarly to ATM-depleted fibroblasts (Fig. 14), also A-T cells are hypersensitive to proteasome inhibition.

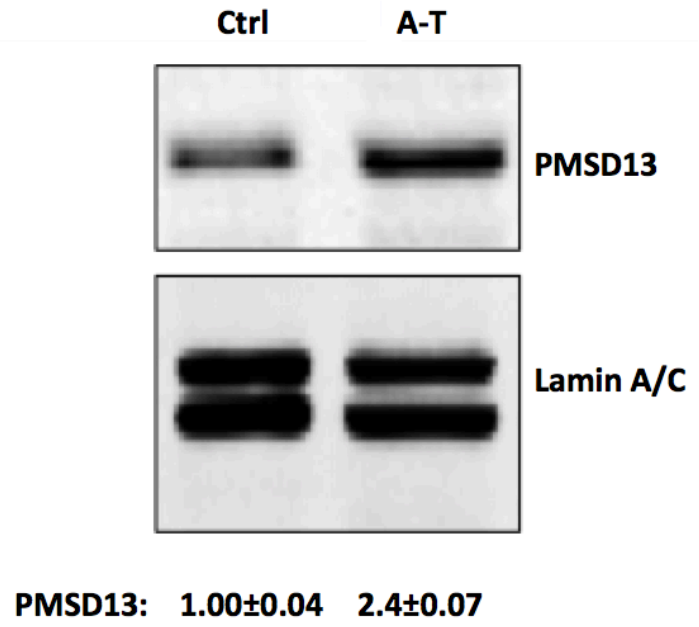


Fig.26 Western blot data demonstrating that A-T fibroblasts display a higher nuclear level of the proteasome subunit PSMD13. 25 µg of cell extracts were loaded on a 12% polyacrylamide gel. Densitometric quantification of the indicated proteins (with the mean ± SD from three independent experiments) is reported at the bottom. Lamin was used as a loading control.

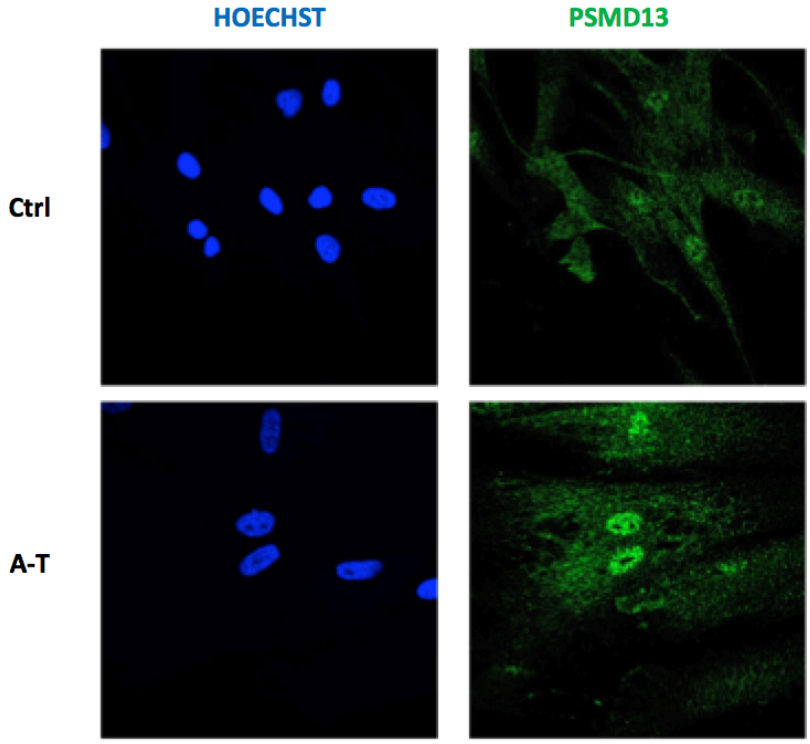


Fig.27 Immunofluorescence micrographs validating the data obtained in **Fig. 26**. Hoechst 33342 was used to stain nuclei.

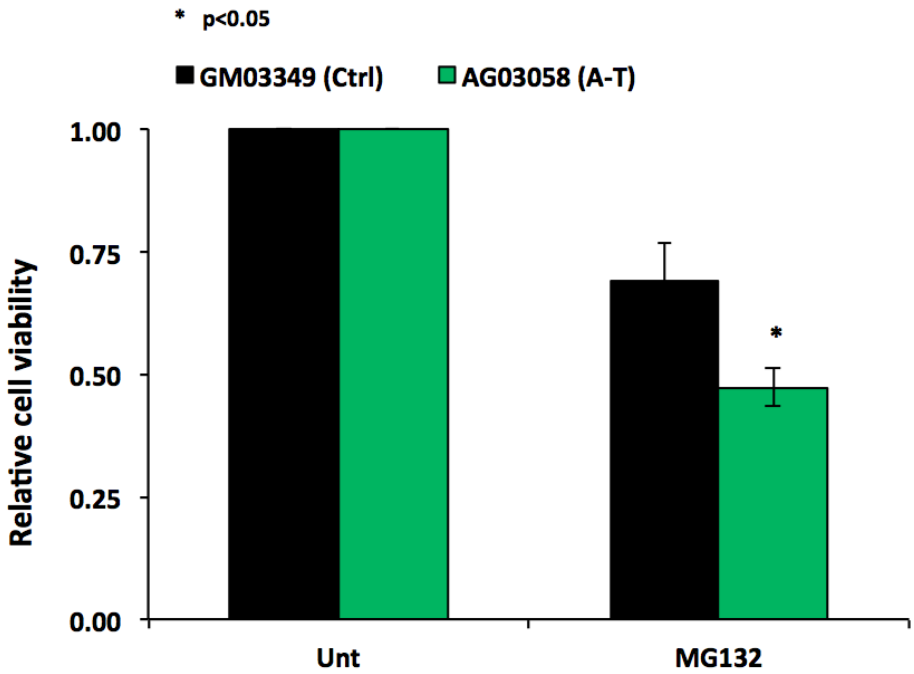
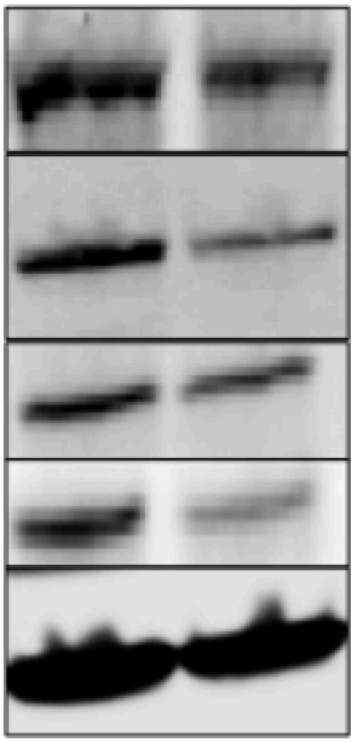


Fig.28 A-T cell sensitivity to proteasome inhibition by MG132 treatment. Cells were incubated with 500 nM MG132 for 24 hours. Viability was measured using the Trypan Blue exclusion assay. The histogram displays the mean with ± SD obtained from three independent experiments. (* p<0.05).

2.5.3 BER components are downregulated in A-T fibroblasts

In order to understand whether the BER pathway is also affected in A-T fibroblasts, we analysed a subset of BER components in these cells. Interestingly, we observed by Western blot that A-T fibroblasts showed lower levels of BER components than healthy cells (Fig. 29), which is in accordance with the results obtained using ATM-depleted fibroblasts (Fig. 16).



XRCC1:	1.00±0.03	0.62±0.02
LigIII:	1.00±0.07	0.80±0.04
PNKP:	1.00±0.01	0.61±0.04
APE1:	1.0±0.03	0.4±0.02

Fig.29 Western blot analysis showing downregulation of BER components in A-T cells. Actin was used as a loading control. 40 µg of cell extracts were loaded on a 12% polyacrylamide gel. Densitometric quantification of the indicated proteins (with the mean ± SD from three independent experiments) is reported at the bottom. Actin was used as a loading control.

Altogether, these data demonstrate that A-T fibroblasts display most of the phenotypes we previously observed using transient ATM depletion, including accumulation of oxidative stress and proteolysis upregulation. Additionally, lower expression of BER components was observed, which strongly suggests that A-T fibroblasts could have reduced BER capacity.

3. Discussion

Despite the importance of ATM for a number of signalling pathways, it is clear that cells lacking ATM are perfectly viable. This is highlighted by the fact that A-T patients can survive beyond their second decade (Rothblum-Oviatt et al., 2016) (Crawford et al., 2000) and that ATM knockout is not embryonic lethal in mice (Barlow et al., 1996). This is potentially the result of a number of adaptive mechanisms occurring upon loss of ATM. Understanding these early phenotypical changes is of great significance, as it will help uncover the molecular basis underlying A-T pathogenesis. Unfortunately, A-T has also been described as a DNA damage response syndrome, characterised by extensive genomic instability (Shiloh & Kastan, 2001). For this reason, it is safe to believe that some of the adaptation mechanisms triggered early on by loss of ATM could have been overlooked by earlier studies because of the presence of widespread genomic rearrangements in A-T cells.

In order to observe and characterise the initial changes occurring after ATM loss, our laboratory addressed this issue using a model of short-term ATM depletion in normal human fibroblasts. Our proteomics analysis allowed us to identify a number of phenotypic changes occurring in response to loss of ATM. This thesis validates two major findings of our proteomic analysis, focussing on the emergence of oxidative stress in ATM-depleted cells and on the upregulation of proteasome subunits in the nuclear compartment, occurring after loss of ATM.

3.1 ATM depletion and oxidative stress

One of the most impressive observations in this thesis is that loss of ATM leads to very early accumulation of ROS. Unbalanced redox homeostasis is normally dealt with by triggering antioxidant systems that effectively neutralise excessive ROS (Birben et al., 2012). In line with this, our proteomics analysis demonstrates that ATM-depleted cells promptly activate the antioxidant response by upregulating a number of genes involved in redox homeostasis (Fig. 3). In fact, our FACS data show time-dependent accumulation of ROS in cells lacking ATM (Fig. 5) as well as in A-T fibroblasts (Fig. 24). These results are perfectly in line with existing literature suggesting accumulation of oxidative stress in cells from A-T patients and in ATM knockout animal models (Kamsler et al., 2001) (Reichenbach et al., 2002), and indicate that antioxidant mechanisms are clearly not sufficient to balance the production of ROS in the absence of ATM.

Moreover, ROS have been suggested to be a major feature underlying A-T pathogenesis, leading to multiple symptoms associated with the syndrome. Our data not only support these findings, but also emphasise an early role for oxidative stress in A-T, as this emerges rapidly in response to ATM loss. We hypothesised two mechanisms that potentially drive ATM-lacking cells to develop oxidative stress. On the one hand, ATM acts as a sensor of oxidative stress and maintains a balanced ROS production by modulating signalling pathways involved in the antioxidant response and cellular metabolism (section 1.1.2). On the other hand, ATM also has been suggested to modulate mitochondrial homeostasis (Ambrose & Gatti, 2013) (Eaton et al., 2007) (Ambrose et al., 2007) (Valentin-Vega et al., 2012). This indicates that the ROS in ATM-depleted cells could derive from dysfunctional mitochondria as well as the presence of a generally disrupted ROS homeostasis.

As introduced earlier, ATM knockout mice have been shown to benefit greatly from treatment with antioxidants (section 1.1.5). In light of our data, it is very likely that antioxidant administration could

improve some of the A-T-associated symptoms in patients. In fact, adjuvant treatments using antioxidants are currently in clinical trial for management of A-T (Lavin et al., 2007).

3.2 Modulation of proteolysis counteracts oxidative stress and contributes to the survival of ATM-depleted cells

As a result of ROS generation and induction of the antioxidant response, we observe here that ATM depletion leads to a rapid accumulation of oxidised proteins in the nuclear compartment (Fig. 6). To the best of our knowledge, this is the first report of oxidative protein damage in ATM-depleted cells. ROS can attack virtually every macromolecule in a cell. Proteins are particularly susceptible to oxidative damage; they can be oxidatively modified by ROS, causing conformational change and leading to protein misfolding and dysfunction (Avery, 2011). Misfolded proteins may aggregate and trigger cell apoptosis, therefore it is crucial for cell to eliminate oxidised proteins before they accumulate (Tyedmers et al., 2010). In fact, mammalian cells exhibit only limited direct reversal mechanisms to remove oxidised proteins (Grune et al., 1997). Most oxidised proteins are targeted for elimination via a ubiquitin-dependent mechanism and degraded by the 26S proteasome in an ATP-dependent manner (Lecker et al., 2006). In agreement with increased carbonylated proteins in the nucleus, our data reveal upregulation of both proteasome subunit and proteolytic activity in the nuclear compartment of ATM-depleted cells (Fig. 7 to 9). Therefore modulation of proteolysis is likely to promote protein degradation by the proteasome machinery, in a mechanism that facilitates the elimination of toxic oxidised proteins in the nuclear compartment. Moreover, another very interesting result from our study is that loss of ATM renders cells susceptible to inhibition of proteolytic activity by proteasome inhibitors, such as MG132 and bortezomib (Fig. 14). This observation strongly suggests that reorganisation of proteolysis is part of an adaptive mechanism promoting survival of ATM-depleted cells and preventing cell death in the presence of oxidative stress, in the short-term after loss of ATM.

In addition to our siRNA-based model, accumulation of oxidised proteins (Fig. 25) and upregulation of proteasome subunits (Fig. 26 and 27) in the nuclear compartment was also observed in A-T fibroblasts. These cells also showed hypersensitivity to proteasome inhibition (Fig. 28). Altogether, these observations suggest that while modulation of proteolytic activity is not sufficient to buffer oxidative protein damage in A-T cells, proteolysis is relevant for the survival of cells lacking ATM.

Additionally, our observations highlight a key point for the clinical management of A-T. One prominent feature of A-T is predisposition to cancer and a number of anti-cancer therapies can be particularly harmful to A-T individuals. For instance, radiation therapy should be administrated carefully and with limited dosage to A-T patients, given their radiosensitivity (Rothblum-Oviatt et al., 2016). Crucially, some proteasome inhibitors are currently in clinical use as anti-cancer agents. Bortezomib, for example, has been approved in the U.S and Europe for the treatment of multiple types of cancer, such as mantle cell lymphoma (Adams & Kauffman, 2004) (Pellom & Shanker, 2012). Our data seem to suggest that use of proteasome inhibitors as anti-cancer agents will have to be carefully evaluated in A-T patients, as A-T fibroblasts show significant sensitivity to proteasome inhibitors.

3.3 BER impairment and DNA damage in ATM-depleted cells

3.3.1 Impaired BER and DNA damage in ATM-depleted cells

To counteract oxidative stress induced by ATM depletion, fibroblasts appear to facilitate proteolysis in the nucleus to eliminate toxic oxidised proteins. Despite the short-term beneficial effects of this process, however, unwanted degradation of nuclear proteins appears to arise as a sort of “side effect”. This affects proteins belonging to the BER pathway, which suffer downregulation upon ATM depletion (Fig. 16). In turn, decreased levels of BER components have a negative impact on BER efficiency, resulting in an impaired BER capacity (Fig. 18 to 22).

Being one of the frontline DNA repair systems, BER acts as a critical player in maintaining genome integrity, promoting normal cell functions and survival (Poletto et al., 2016). It is clear that deficiency in BER capacity will lead to spontaneous accumulation of DNA damage (Orlando et al., 2014) (Khoronenkova & Dianov, 2015) (Poletto et al., 2016). Unsurprisingly, ATM-depleted cells display accumulation of different types of spontaneous DNA lesions (Fig. 23). In addition to a diminished BER, it is very likely that ATM-depletion itself will have negative impact on DNA repair capacity as ATM is an important signaling regulator of DDR. In fact, DNA damage in ATM-depleted cells is likely not to be sorely caused by impaired BER. Data from our laboratory have shown a partial rescue of DNA damage in ATM-depleted cells treated with the antioxidant NAC (data not shown). This indicates that, in addition to BER deficiency, ROS generated by ATM depletion might also generate some of the DNA damage measured in ATM-depleted cells. This would add up to the lesions spontaneously accumulated as a consequence of an impaired BER capacity. Therefore, a deficient BER pathway together with accumulation of ROS would give rise to a substantial amount of DNA damage in ATM-depleted cells, which will accumulate and eventually promote genomic instability.

3.3.2 Is BER deficiency associated with A-T pathogenesis?

A-T is a genomic instability syndrome (Shiloh & Kastan, 2001). Previous studies have shown that loss of functional ATM impacts the G_1/S cell cycle checkpoints, resulting in uncontrolled replication of damaged DNA and genomic instability (Shiloh & Ziv, 2013) (Khoronenkova & Dianov, 2015). The work reported in this thesis indicates that BER impairment could be at least partially responsible for the genomic instability typical of A-T. Loss of ATM leads to BER impairment and spontaneously occurring DNA damage will start to accumulate. At the same, as cell cycle checkpoints are negatively affected by the absence of ATM, cells are not able to arrest in G_0/G_1 but will entry S phase, where replication of DNA over SSBs drives generation of DSBs. As DNA repair capacity and signaling of DNA damage are simultaneously impaired in ATM-depleted cells, DSBs will accumulate and eventually

trigger genomic instability. This suggests a novel mechanistic explanation for the pathogenesis of A-T associated cancer predisposition, whereby an impaired BER pathway could potentially constitute one of the early mechanisms promoting the development of chromosomal instability in cells lacking ATM. Furthermore, deficiency in BER activity could also be linked to neurodegeneration, yet another hallmark of A-T. In fact, a very recent study identified a patient displaying cerebellar ataxia in association with severely reduced expression of XRCC1 (Hoch et al., 2017). As cerebellar ataxia is a typical hallmark of A-T, this report suggests that BER homeostasis could contribute to A-T-related neurological dysfunction.

3.4 Strengths, limitations and conclusions of this study

3.4.1 Strengths and limitations of our approach

Our study bears a number of strengths and substantial novelty. Firstly, in this report we made use of human diploid fibroblasts. Our experimental model is very informative, when compared with previous studies that used transformed cells, as cell transformation can considerably affect the gene expression pattern and bias the interpretation of experimental data. For example, an early study addressing BER capacity in A-T individuals was carried out using lymphoblasts and concluded that A-T patients have unchanged BER efficiency (Cappelli et al., 2000). While cell type-specific variations may exist, it is worth highlighting that the lymphoblast cells used by Cappelli et al. were transformed using the Epstein-Barr virus (Cappelli et al., 2000). Previous work from our laboratory has shown that viral transformation can have a significant impact on the expression and coordination of BER enzymes (Poletto et al., 2016). Another advantage of our study is that we used a temporary depletion model to analyse the early changes occurring upon ATM depletion. As mentioned before, ATM dysfunction typically leads to genomic instability; therefore it is plausible that some immediate changes in gene/protein expression could have been overlooked by previous studies. Our experimental model focussed on a narrow window prior to the onset of genetic instability, which sheds light on the adaptive mechanisms in response to ATM loss. Finally, our study based on SILAC

proteomics allowed us to focus on the early changes occurring in the absence of ATM in a completely unbiased manner.

Despite the evident advantages of our study, our approach has some drawbacks. Cells used in this report are human fibroblasts; while we validated most of the phenotypes using A-T fibroblasts, the situation is much more complicated in a patient where all cell types have impaired ATM expression. Cells more relevant to the A-T pathology, such as neuron cells or lymphoblasts, could potentially behave differently in response to a loss of ATM. Therefore, although the data presented this study are extremely valuable, other cell types should be analysed in order to reach definitive conclusions regarding A-T pathogenesis. Additionally, this report mainly focuses on the BER pathway in the context of ATM depletion. It is very likely that, as a consequence of increased nuclear proteolysis, other DNA repair and metabolic pathways could also be negatively influenced by the loss of ATM. These mechanisms could also contribute to the phenotype, such as accumulation of DNA damage, observed in ATM-depleted cells.

3.4.2 Conclusions

Our study investigates changes occurring very early on upon loss of ATM in human cells. A schematic summary of our findings is depicted in Fig. 30. This study confirms previous observations linking loss of ATM to accumulation of oxidative stress. Our data show that the first, short-term response to oxidative stress aims to protect proteins from excessive oxidation. To this end, upregulation of nuclear proteolysis is a very effective adaptive mechanism that contributes to cell survival at early stages after loss of ATM. Meanwhile, increased nuclear proteolysis has an inevitable impact on nuclear proteins, including the BER components. We assume that accumulation of DNA damage is not an immediate concern for cells in the short-term after loss of ATM, because absence of such an important signalling molecule makes it probably impossible for cells to even sense DNA damage at this stage. For this reason we conclude that proteolysis efficiently promotes cell survival in the

presence of oxidative stress at early stages after ATM loss. However, deficiencies in DNA repair due to modulation of proteolysis and DDR signals due to loss of ATM will lead to accumulation of spontaneous DNA strand breaks, and eventually development of genomic instability in a long-term.

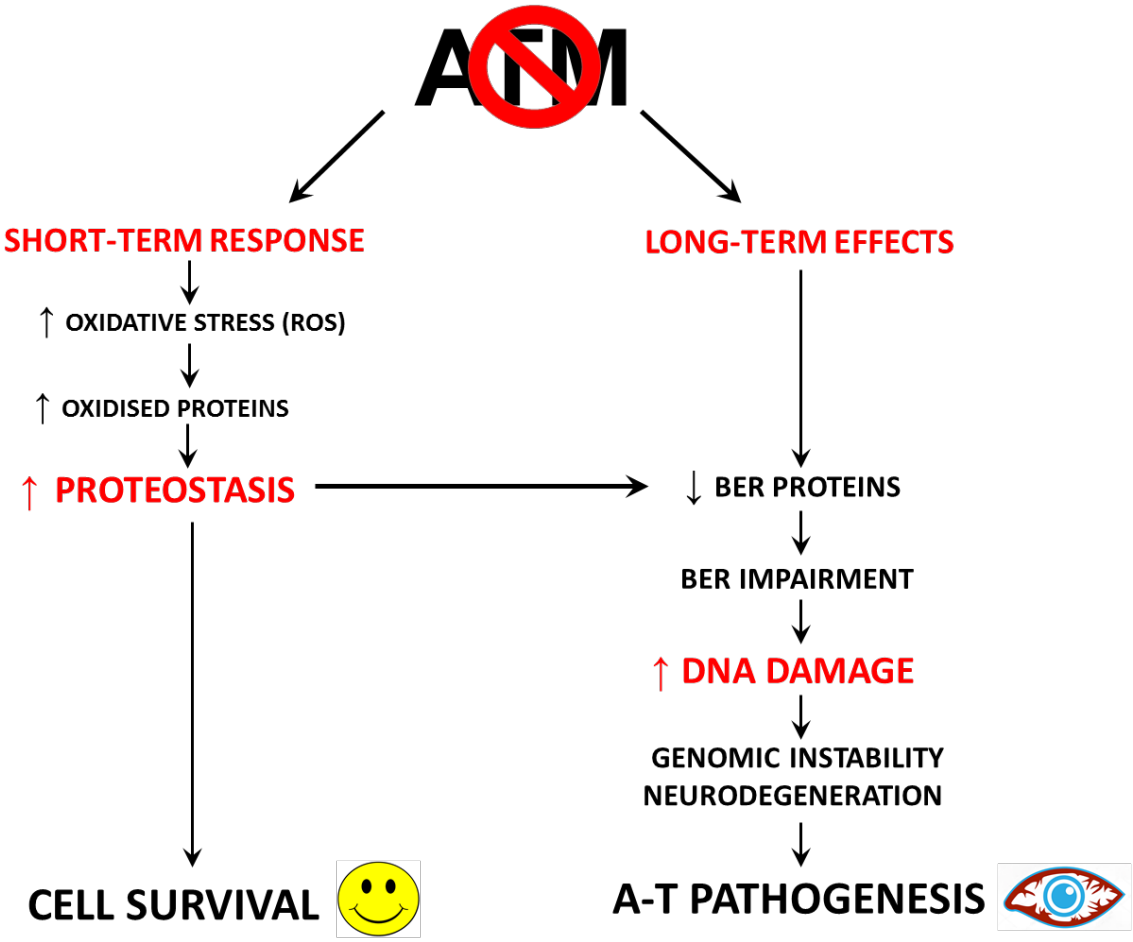


Fig.30 Schematic diagram of the model supported by this study. Loss of functional ATM leads to immediate induction of oxidative stress. In an effort to adapt to persistent ROS, cells upregulate proteolysis that counteracts protein oxidative damage and promotes cell survival in the absence of ATM. However, increased proteolysis inevitably causes downregulation of BER proteins and results in an impaired BER capacity in the long-term. Spontaneous DNA strand breaks accumulate, which drive the development of A-T-associated features such as genomic instability and neurodegeneration.

4. Material and methods

4.1 Materials

4.1.1 List of the antibodies used in this study.

Antibody	Reactivity	Clonality	Dilution	Application	Source
Anti-α-tubulin	Mouse	Monoclonal	1:10000	Western blot	Sigma Aldrich
Anti-β-actin	Mouse	Monoclonal	1:10000	Western blot	Abcam
Anti-APE1	Rabbit	Polyclonal	1:5000	Western blot	Novus Biologicals
Anti-ATM	Mouse	Monoclonal	1:2000	Western blot	Sigma Aldrich
Anti-DNP	Rabbit	Polyclonal	1:10000	Western blot	Abcam
Anti-Ku80	Mouse	Monoclonal	1:2000	Western blot	Abcam
Anti-Hsp90	Rabbit	Polyclonal	1:2000	Western blot	Abcam
Anti-Lamin A/C	Rabbit	Monoclonal	1:10000	Western blot	Abcam
Anti-LigIII	Rabbit	Polyclonal	1:1000	Western blot	Made in house
Anti-PNKP	Rabbit	Polyclonal	1:2000	Western blot	Gift from Prof. Michael Weinfeld (University of Alberta)
Anti-PSMA5	Rabbit	Polyclonal	1:5000	Western blot	Cell Signaling Technology
Anti-PSMB5	Rabbit	Polyclonal	1:500	Western blot	Abcam
Anti-PSMD13	Rabbit	Polyclonal	1:1000	Western blot/ Immunofluorescence	Proteintech
Anti-Sp1	Rabbit	Polyclonal	1:2000	Western blot	Millipore
Anti-XRCC1	Mouse	Monoclonal	1:5000	Western blot	Thermo Scientific
AlexaFluor 680	Mouse	Polyclonal	1:10000	Western blot	Molecular Probes
IRDye® 800	Rabbit	Polyclonal	1:10000	Western blot/	Rockland
Alexa 488	Rabbit	Polyclonal	1:250	Immunofluorescence	ThermoFisher

4.1.2 List of the siRNA sequences used in this study.

Gene	Sequence
Negative control	Eurogentec - proprietary sequence.
53BP1	5’-CAGGACAGUCUUUCCACGAAU-3’
APE1	5'-AAUGACAAAGAGGCAGCAGG-3'
ATM #1	5'-AACAUACUACUCAAAGACAUU-3'

ATM #2	5'- UGGUGCUAUUUACGGAGCU -3'
ATM #3	5'- GCGCCUGAUUCGAGAUCCU -3'
LigIII	5'-AACUGCAACCCAGAUGAUAUG-3'
RNF20	5'-CCAAUGAAAUCAAGUCUAAUU-3'

4.2 Methods

4.2.1 Cell culture and siRNA transfections

Human diploid fibroblasts (TIG-1) were obtained from the Coriell Cell repository and grown in Dulbecco's modified Eagle's medium (DMEM) (Invitrogen), supplemented with 15% (v/v) foetal bovine serum (FBS) at 37℃ with 5% (v/v) CO_2. A-T (AG03058) and heathy (GM03349) fibroblasts were also obtained from Coriell and were grown in the same conditions.

siRNA transfections were performed using the Lipofectamine RNAiMAX reagent (Invitrogen) according to the manufacturer's instructions. For siRNA transfections, 30 nM siRNA and 10 µl Lipofectamine were separately incubated with 500 µl FBS-free DMEM for 5 minutes at room temperature. Then, siRNA and Lipofectamine were mixed together and further incubated for 15 minutes at room temperature, prior to addition to cells. Cells were incubated with siRNAs for the indicated time before harvest. For simultaneous transfection of BER and ATM siRNAs, a sequential approach was employed. 30 nM ATM siRNA was firstly transfected into cells. 24 hours later, 5 nM of the BER siRNA (either the APE1 or LigIII) was added. 48 hours later cells were harvested. The total time with each siRNA was 72 hours for ATM and 48 hours for BER-specific siRNAs. This approach allowed us to achieve a mild depletion of BER proteins, which was comparable with the downregulation observed in ATM-depleted cells.

4.2.2 Stable isotope labelling with amino acids in cell culture (SILAC) and mass spectrometry

SILAC experiments were performed essentially as described in (Markkanen et al., 2015). TIG-1 cells were transfected with either a control or an ATM-targeting siRNA, and grown in "light" R_0K_0 (siCtrl) or "heavy" $R_{10}K_8$ (siATM) medium, respectively. Arginine and lysine were labelled with the isotopes ^{13}C and ^{15}N in the "heavy" medium. Seventy-two hours after transfection cells were counted and mixed in a 1:1 ratio and subjected to fractionation into cytoplasmic and nuclear extracts as described below. Protein extracts were then alkylated and precipitated using chloroform/methanol and sequentially digested into peptides using immobilised trypsin. Digested samples were desalted and subjected to analysis by nano-ultraperformance liquid chromatography tandem mass spectrometry (nUPLC-MS/MS) at the Target Discovery Institute (University of Oxford).

4.2.3 Generation of cell extracts

Whole cell extracts (WCEs) were prepared using a modified version of the original method from Tanaka and colleagues (Tanaka et al., 1992). Cells were harvested by centrifugation at 350 relative centrifugal force (rcf) for 3 minutes at 4 ℃. Cell pellets were then resuspended in one packed cell volume (PCV) of cold buffer containing 10 mM Tris–HCl pH 7.8, 200 mM KCl and 1 μg/ml of each protease inhibitor (pepstatin, aprotinin, chymostatin and leupeptin), 1 mM N-ethylmaleimide (NEM), 1 mM phenylmethanesulfonyl fluoride (PMSF) and 1mM dithiothreitol *(*DTT). Cell suspension was then lysed in two PCV of cold buffer containing 10 mM Tris–HCl pH 7.8, 600 mM KCl, 40% (v/v) glycerol, 2 mM ethylenediaminetetraacetic acid (EDTA), 0.2% (v/v) Nonidet P-40 and 1 μg/ml of each protease inhibitor, 1 mM NEM, 1 mM PMSF and 1 mM DTT. Cells were rocked for 20 minutes at 4 ℃. Then, the cell lysate was centrifuged at 16000 rcf at 4 ℃ for 30 minutes. The supernatant was collected and used as WCE.

Cytoplasmic/nuclear fractions were generated using a protocol developed in our lab. Briefly, cell pellets were resuspended in two PCV of cold buffer I containing 20 mM Tris–HCl pH 7.8, 2.5 mM $MgCl_2$, 0.5% (v/v) Nonidet P-40, 1 mM NEM, 1 mM PMSF, 1 mM DTT and 1 µg/ml of each protease inhibitor. After a 10-minute incubation on ice, nuclei precipitated by centrifugation at 10000 rcf for 2 minutes. The supernatant, containing the cytoplasmic extract, was then collected. The nuclear cell pellet was then resuspended in two PCV of cold buffer II containing 20 mM Tris–HCl pH 8.0, 500 mM NaCl, 1 mM EDTA, 0.75% (v/v) Triton X-100, 10% (v/v) glycerol, 5 mM MgCl2, 1mM NEM, 1mM PMSF, 1mM DTT and 1 µg/ml of each protease inhibitor. After 10-minutes incubation on ice, insoluble DNA components were separated by centrifugation at 10000 rcf for 2 minutes. The supernatant (i.e. the nuclear fraction) was transferred to a fresh tube.

Protein concentration was determined using a Bradford assay (Bio-Rad), using bovine serum albumin (BSA) to generate a standard curve.

4.2.4 Sodium dodecyl sulphate polyacrylamide gel electrophoresis (SDS-PAGE) and Western blot

Proteins were separated using SDS-PAGE. Polyacrylamide gels were made in house varying the acrylamide percentage as needed (from 8 to 16% (v/v)), or using gradient gels (4-16% (v/v) acrylamide). Before samples loading, they were denatured by into a loading buffer containing 12 mM Tris-HCl pH 6.8, 0.4% (w/v) SDS, 2% (v/v) glycerol, 1% (v/v) β-mercaptoethanol and 0.05% (w/v) bromophenol blue. Electrophoresis was performed in Tris/glycine/SDS (TGS) running buffer containing 25 mM Tris-HCl pH 8.3, 192 mM glycine and 0.1% (w/v) SDS.

Proteins were transferred to polyvinylidene fluoride (PVDF) membranes. Transfer was carried out in Tris/glycine (TG) buffer containing 192 mM glycine, 25 mM Tris-HCl pH 8.3 and 20% (v/v) methanol at 25 V for 3 hours at room temperature. Prior to incubation with primary antibodies, membranes were saturated with Odyssey blocking buffer (Li-cor Biosciences) for 1 hour at room temperature.

Then membranes were incubated with the relevant primary antibody diluted in Odyssey blocking buffer with 0.1% (v/v) Tween-20. Membranes were washed three times for 5 minutes in phosphate-buffer saline (PBS) (Sigma) containing 0.1% (v/v) Tween-20. Fluorophore-conjugated secondary antibodies conjugated were incubated with membranes for at least 1 hour. Finally, membranes were washed three times with PBS supplemented with 0.1% (v/v) Tween-20. Proteins were detected and quantified using an Odyssey image analysis system (Li-Cor Biosciences).

4.2.5 Detection of protein carbonylation

Protein carbonylation was assessed using the Oxidized Protein Western Blot Kit (AbCam). Cells were fractionated as described above to generate cytoplasmic and nuclear extracts. 10 μg of cell extract was denatured in 6% (w/v) SDS, incubated with a 2,4-dinitrophenylhydrazine (2,4-DNP) solution provided with the kit for 1 minute at room temperature. The reaction was stopped by adding the provided Neutralisation Solution, protein samples were subsequently separated by SDS-PAGE. DNP-derivatised carbonyl adducts were detected through Western blot using the anti-DNP primary antibody provided with the kit, followed by an IRDye® 800-conjugated secondary antibody.

For ROS quantification, cells were harvested by trypsinisation and collected by centrifugation at 500 rcf for 3 minutes. Cell pellets were subsequently resuspended in PBS containing 10 μM H2DCFDA and incubated for 30 minutes at 37 °C. The fluorescent intensity of the dye was measured using a Becton-Dickinson FACSCalibur™ system. The relative ROS content was determined by calculating the ratio between H2DCFDA and forward scatter to correct for cell size.

4.2.6 Immunostaining

Immunostaining was carried out following standard procedures. Briefly, after treatment with the relevant siRNA cells were fixed with 4% (v/v) paraformaldehyde in PBS for 15 minutes. Then, cells

were permeabilised in cold 0.2% (v/v) Triton X-100 in PBS for 15 minutes. Cells were then saturated in 5% (w/v) BSA in PBS at room temperature for 1 hour. Primary antibodies were incubated in PBS supplemented with 0.01% (v/v) Tween 20. The secondary antibody was Alexa Fluor 488 (H+L)-conjugated (Life Technologies). Nuclei were stained using Hoechst 33342 (Life Technologies). Cell images were acquired using a 710 confocal laser scanning microscopy (Zeiss), quantification was performed using the ImageJ software.

4.2.7 *In vitro* proteasome and BER assays

Proteasome activity was determined using an assay originally designed to detect chymotrypsin-like activity, as described in (Arlt et al., 2009). Cells were lysed to generate cytoplasmic and nuclear extracts as described above, taking care to omit any protease inhibitor. Cell lysates were adjusted to equal protein concentration prior to use. To assess the proteasome chymotrypsin-like activity, 1μg of cytoplasmic extract or 5 μg of nuclear extract was incubated in 100 mM Tris-HCl pH 8.0, 10 mM $MgCl_2$, 2 mM ATP supplemented with 50 μM of a Suc-LLVY-AMC (AMC - R&D Systems) substrate at 37 °C for 50 minutes. The fluorescent emission of cleaved AMC was detected using a POLARstar Omega plate reader (BMG Labtech) with excitation/emission wavelengths of 380 nm/460 nm. Proteasome-specific chymotrypsin activity was determined by subtracting any proteasome-independent proteolytic activity from identical reactions run in parallel in presence of 10 μM MG132. *In vitro* BER assays were performed essentially as described in (McNeill et al., 2004). For AP site incision assays, the DNA substrate used was a tetrahydrofuran (THF)-containing oligonucleotide, 5′-AATTCACCGGTACG(THF)TCTAGAATTCG-3′, 5′ labelled with IRDye®800 (IDT) and annealed to a complementary DNA sequence 5′-CGAATTCTAGA(C)CGTACCGGTGAATT-3’. Incorporation of THF in the DNA template mimics the morphology of a natural AP site, which can be recognised by APE1. A schematic diagram of the reaction is illustrated in Fig. 31. For the assay, 50 ng of whole cell extract was incubated in 25 mM Tris-HCl pH 7.4, 1 mM $MgCl_2$, 100 mM KCl, 1 mM DTT at 37 °C in the

presence of 50 nM DNA substrate for the indicated time (5-20 minutes). The reaction was stopped by adding 10 µl of a buffer containing 96% (v/v) formamide and 10 mM EDTA.

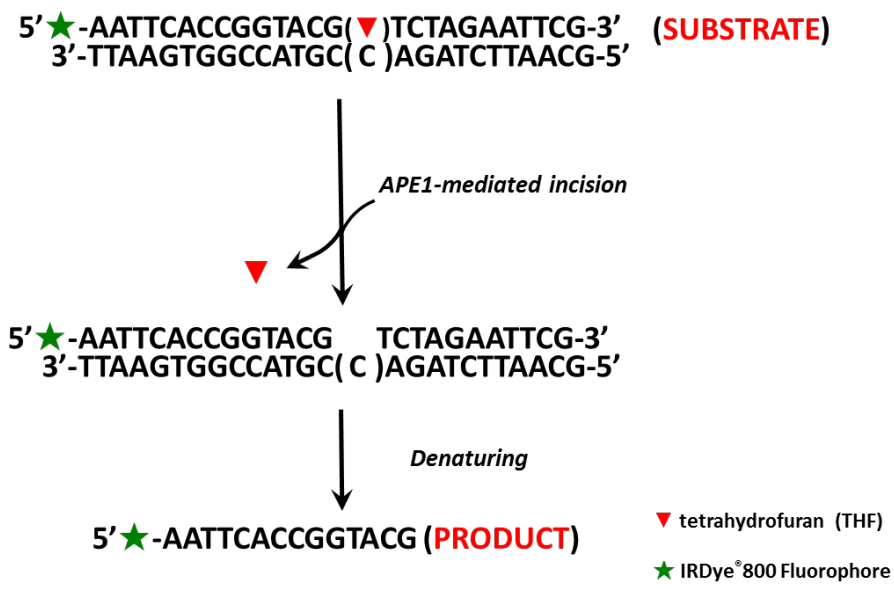


Fig.31 Schematic illustration of the *in vitro* AP-site incision assay.

For nick ligation assays, the DNA substrate used was a 5'-labelled nick-containing oligonucleotide, 5´-AATTCACCGGTACGG(OH)(P)TCTAGAATTCG-3´, where (OH) is an hydroxyl moiety and (P) is a phosphate moiety. The substrate was annealed to the same complementary sequence used in the AP site incision assays. 2.5 µg of nuclear extract and 50 nM DNA substrate were incubated in 50 mM Tris-HCl pH 7.5, 10 mM $MgCl_2$, 10 mM DTT, 1 mM ATP at 25 °C for the indicated time. The reaction was stopped as described above.

For both assays, oligonucleotides were separated using a 20% (v/v) denaturing polyacrylamide gel containing 7 M urea. Samples were detected and quantified using Odyssey image analysis system (Li-Cor Biosciences). A schematic diagram of the reaction is illustrated in Fig. 32.

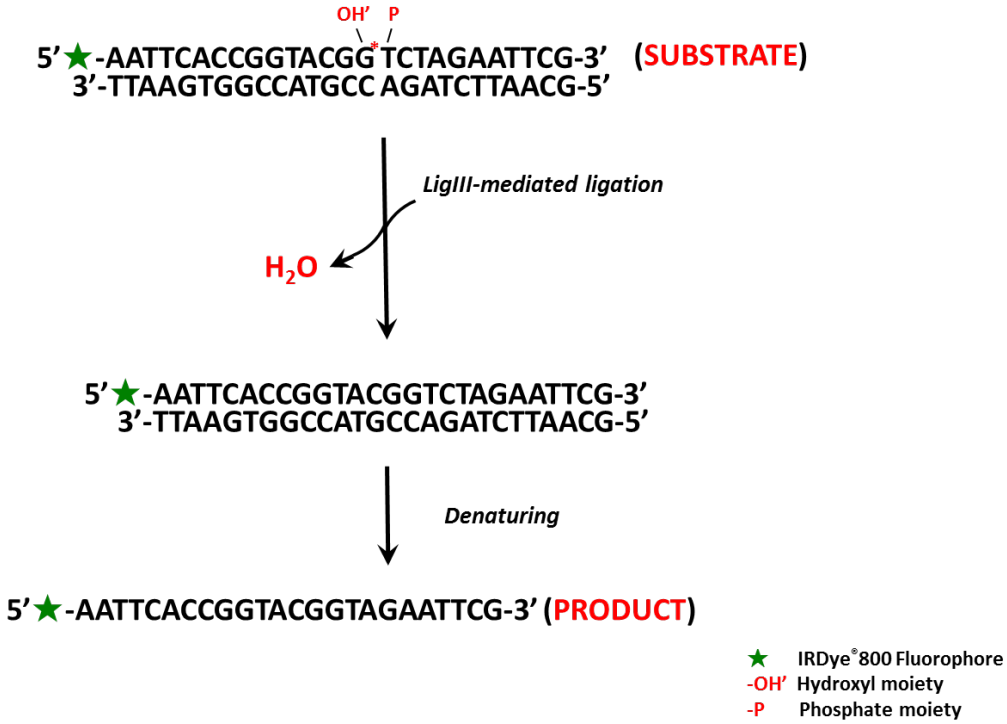


Fig.32 Schematic illustration of the *in vitro* nick ligation incision assay.

4.2.8 Comet assays

Alkaline and neutral comet assays were performed as previously described (Parsons et al., 2009) (Wojewodzka et al., 2002). For alkaline comet assay, upon transfection with the appropriate siRNA, cells were trypsinised and transferred to a 24-well plate (5.0 x 10^4 cells/ well). The cell suspension was mixed with 1% (w/v) low-melting point agarose in 1 X PBS and embedded on a microscope slide (Bio-Rad). Cells were lysed in a buffer containing 2.5 M NaCl, 10 mM Tris pH 10.5, 100 mM EDTA, 300 mM NaOH, 1% (v/v) dimethylsulphoxide (DMSO) and 1% (v/v) Triton X-100, for 1 hour at 4 °C. Before electrophoresis, the slides were placed in a buffer containing 300mM NaOH, 1 mM EDTA, 1% (v/v) DMSO (pH> 13), and incubated protected from light for 30 minutes to allow DNA to unwind. Slides were electrophoresed for 25 minutes at 25 V (300 mA). After electrophoresis, slides were washed with 0.4 M Tris pH 7.5 three times for neutralisation.

For neutral comet assay, after cells were embedded on the slides with agarose, they were lysed in 2.5 M NaCl, 10 mM Tris pH 9.5, 100 mM EDTA, 1% (v/v) sodium lauryl sarcosinate, 1% (v/v) DMSO

and 1% (v/v) Triton X-100, for 2 hours at 4 °C. Slides were rinsed three times in Tris/borate/EDTA (TBE) before electrophoresing in TBE buffer at 25 V for 25 minutes.

4.2.9 Statistical analyses

All the experiments were run with the appropriate amount of technical replicates. Data are presented as mean ± SD obtained from at least three independent biological experiments. p values were calculated using the Student's two-tailed t test for normally distributed datasets using Microsoft Excel.

References

Adams, J., & Kauffman, M. (2004). Development of the proteasome inhibitor Velcade (Bortezomib). *Cancer Investigation*, *22*(2), 304–311.

Alexander, A., Cai, S.-L., Kim, J., Nanez, A., Sahin, M., MacLean, K. H., … Walker, C. L. (2010). ATM signals to TSC2 in the cytoplasm to regulate mTORC1 in response to ROS. *Proceedings of the National Academy of Sciences of the United States of America*, *107*(9), 4153–4158.

Ambrose, M., & Gatti, R. A. (2013). Pathogenesis of ataxia-telangiectasia: the next generation of ATM functions. *Blood*, *121*(20), 4036–4045.

Ambrose, M., Goldstine, J. V, & Gatti, R. A. (2007). Intrinsic mitochondrial dysfunction in ATM-deficient lymphoblastoid cells. *Human Molecular Genetics*, *16*(18), 2154–2164.

Anheim, M., Tranchant, C., & Koenig, M. (2012). The autosomal recessive cerebellar ataxias. *The New England Journal of Medicine*, *366*(7), 636–646.

Arlt, A., Bauer, I., Schafmayer, C., Tepel, J., Muerkoster, S. S., Brosch, M., … Schafer, H. (2009). Increased proteasome subunit protein expression and proteasome activity in colon cancer relate to an enhanced activation of nuclear factor E2-related factor 2 (Nrf2). *Oncogene*, *28*(45), 3983–3996.

Avery, S. V. (2011). Molecular targets of oxidative stress. *The Biochemical Journal*, *434*(2), 201–210.

Bagley, J., Singh, G., & Iacomini, J. (2007). Regulation of oxidative stress responses by ataxia-telangiectasia mutated is required for T cell proliferation. *Journal of Immunology (Baltimore, Md. : 1950)*, *178*(8), 4757–4763.

Barlow, C., Hirotsune, S., Paylor, R., Liyanage, M., Eckhaus, M., Collins, F., … Wynshaw-Boris, A. (1996). Atm-Deficient Mice: A Paradigm of Ataxia Telangiectasia. *Cell*, *86*(1), 159–171.

Barzilai, A., Rotman, G., & Shiloh, Y. (2002). ATM deficiency and oxidative stress: a new dimension of defective response to DNA damage. *DNA Repair*, *1*(1), 3–25.

Beal, M. F. (2002). Oxidatively modified proteins in aging and disease. *Free Radical Biology & Medicine*, *32*(9), 797–803.

Birben, E., Sahiner, U. M., Sackesen, C., Erzurum, S., & Kalayci, O. (2012). Oxidative Stress and Antioxidant Defense. *The World Allergy Organization Journal*, *5*(1), 9–19.

Biton, S., Barzilai, A., & Shiloh, Y. (2008). The neurological phenotype of ataxia-telangiectasia: solving a persistent puzzle. *DNA Repair*, *7*(7), 1028–1038.

Bonvini, P., Zorzi, E., Basso, G., & Rosolen, A. (2007, April). Bortezomib-mediated 26S proteasome inhibition causes cell-cycle arrest and induces apoptosis in CD-30+ anaplastic large cell lymphoma. *Leukemia*. England.

Bredemeyer, A. L., Sharma, G. G., Huang, C.-Y., Helmink, B. A., Walker, L. M., Khor, K. C., … Sleckman, B. P. (2006). ATM stabilizes DNA double-strand-break complexes during V(D)J recombination. *Nature*, *442*(7101), 466–470.

Broeks, A., Urbanus, J. H. M., Floore, A. N., Dahler, E. C., Klijn, J. G. M., Rutgers, E. J. T., … van 't Veer, L. J. (2000). ATM-Heterozygous Germline Mutations Contribute to Breast Cancer–Susceptibility .

American Journal of Human Genetics, *66*(2), 494–500.

Brown, J. S., & Jackson, S. P. (2015). Ubiquitylation, neddylation and the DNA damage response. *Open Biology*, *5*(4), 150018.

Bus, J. S., & Gibson, J. E. (1984). Paraquat: model for oxidant-initiated toxicity. *Environmental Health Perspectives*, *55*, 37–46.

Cabana, M. D., Crawford, T. O., Winkelstein, J. A., Christensen, J. R., & Lederman, H. M. (1998). Consequences of the delayed diagnosis of ataxia-telangiectasia. *Pediatrics*, *102*(1 Pt 1), 98–100.

Caldecott, K. W. (2008). Single-strand break repair and genetic disease. *Nature Reviews. Genetics*, *9*(8), 619–631.

Caldecott, K. W., McKeown, C. K., Tucker, J. D., Ljungquist, S., & Thompson, L. H. (1994). An interaction between the mammalian DNA repair protein XRCC1 and DNA ligase III. *Molecular and Cellular Biology*, *14*(1), 68–76.

Cappelli, E., Rossi, O., Chessa, L., & Frosina, G. (2000). Efficient DNA base excision repair in ataxia telangiectasia cells. *European Journal of Biochemistry*, *267*(23), 6883–6887.

Cappelli, E., Taylor, R., Cevasco, M., Abbondandolo, A., Caldecott, K., & Frosina, G. (1997). Involvement of XRCC1 and DNA Ligase III Gene Products in DNA Base Excision Repair. *Journal of Biological Chemistry* , *272*(38), 23970–23975. https://doi.org/10.1074/jbc.272.38.23970

Chen, D. S., Herman, T., & Demple, B. (1991). Two distinct human DNA diesterases that hydrolyze 3'-blocking deoxyribose fragments from oxidized DNA. *Nucleic Acids Research*, *19*(21), 5907–5914.

Chou, W.-C., Hu, L.-Y., Hsiung, C.-N., & Shen, C.-Y. (2015). Initiation of the ATM-Chk2 DNA damage response through the base excision repair pathway. *Carcinogenesis*, *36*(8), 832–840.

Chun, H. H., Sun, X., Nahas, S. A., Teraoka, S., Lai, C. H., Concannon, P., & Gatti, R. A. (2003). Improved diagnostic testing for ataxia-telangiectasia by immunoblotting of nuclear lysates for ATM protein expression. *Molecular Genetics and Metabolism*, *80*(4), 437–443.

Chussil, J. (1992). Sclerotherapy treatment of varicose and telangiectatic leg veins. *Archives of Dermatology*, *128*(3), 426.

Collins, A. R., Oscoz, A. A., Brunborg, G., Gaivao, I., Giovannelli, L., Kruszewski, M., … Stetina, R. (2008). The comet assay: topical issues. *Mutagenesis*, *23*(3), 143–151.

Cooke, M. S., Evans, M. D., Dizdaroglu, M., & Lunec, J. (2003). Oxidative DNA damage: mechanisms, mutation, and disease. *FASEB Journal : Official Publication of the Federation of American Societies for Experimental Biology*, *17*(10), 1195–1214.

Crawford, T. O., Mandir, A. S., Lefton-Greif, M. A., Goodman, S. N., Goodman, B. K., Sengul, H., & Lederman, H. M. (2000). Quantitative neurologic assessment of ataxia-telangiectasia. *Neurology*, *54*(7), 1505–1509.

Crawford, T. O., Skolasky, R. L., Fernandez, R., Rosquist, K. J., & Lederman, H. M. (2006). Survival probability in ataxia telangiectasia. *Archives of Disease in Childhood*, *91*(7), 610–611.

D'Souza, A. D., Parish, I. A., Krause, D. S., Kaech, S. M., & Shadel, G. S. (2013). Reducing Mitochondrial ROS Improves Disease-related Pathology in a Mouse Model of Ataxia-telangiectasia. *Molecular Therapy*, *21*(1), 42–48.

Dalle-Donne, I., Rossi, R., Giustarini, D., Milzani, A., & Colombo, R. (2003). Protein carbonyl groups as biomarkers of oxidative stress. *Clinica Chimica Acta; International Journal of Clinical Chemistry*, *329*(1–2), 23–38.

Davies, M. J. (2016). Protein oxidation and peroxidation. *Biochemical Journal*, *473*(7), 805 LP-825.

Dianov, G. L., & Hübscher, U. (2013). Mammalian Base Excision Repair: the Forgotten Archangel. *Nucleic Acids Research*, *41*(6), 3483–3490.

Driessen, G. J., Ijspeert, H., Weemaes, C. M. R., Haraldsson, A., Trip, M., Warris, A., … van der Burg, M. (2013). Antibody deficiency in patients with ataxia telangiectasia is caused by disturbed B- and T-cell homeostasis and reduced immune repertoire diversity. *The Journal of Allergy and Clinical Immunology*, *131*(5), 1367–75.e9.

mutated kinase regulates ribonucleotide reductase and mitochondrial homeostasis. *The Journal of Clinical Investigation*, *117*(9), 2723–2734.

Espinosa-Diez, C., Miguel, V., Mennerich, D., Kietzmann, T., Sanchez-Perez, P., Cadenas, S., & Lamas, S. (2015). Antioxidant responses and cellular adjustments to oxidative stress. *Redox Biology*, *6*, 183–197.

Feigin, R. D., Vietti, T. J., Wyatt, R. G., Kaufman, D. G., & Smith, C. H. J. (1970). Ataxia telangiectasia with granulocytopenia. *The Journal of Pediatrics*, *77*(3), 431–438.

Frosina, G., Fortini, P., Rossi, O., Carrozzino, F., Raspaglio, G., Cox, L. S., … Dogliotti, E. (1996). Two pathways for base excision repair in mammalian cells. *The Journal of Biological Chemistry*, *271*(16), 9573–9578.

Gatti, R. A., Boder, E., Vinters, H. V, Sparkes, R. S., Norman, A., & Lange, K. (1991). Ataxia-telangiectasia: an interdisciplinary approach to pathogenesis. *Medicine*, *70*(2), 99–117.

Gilmore, E. C. (2014). DNA repair abnormalities leading to ataxia: shared neurological phenotypes and risk factors. *Neurogenetics*, *15*(4), 217–228.

Grune, T., Reinheckel, T., & Davies, K. J. (1997). Degradation of oxidized proteins in mammalian cells. *FASEB Journal : Official Publication of the Federation of American Societies for Experimental Biology*, *11*(7), 526–534.

Guo, Z., Deshpande, R., & Paull, T. T. (2010). ATM activation in the presence of oxidative stress. *Cell Cycle*, *9*(24), 4805–4811.

Guo, Z., Kozlov, S., Lavin, M. F., Person, M. D., & Paull, T. T. (2010). ATM activation by oxidative stress. *Science (New York, N.Y.)*, *330*(6003), 517–521.

Herzog, K. H., Chong, M. J., Kapsetaki, M., Morgan, J. I., & McKinnon, P. J. (1998). Requirement for Atm in ionizing radiation-induced cell death in the developing central nervous system. *Science (New York, N.Y.)*, *280*(5366), 1089–1091.

Higurashi, M., & Conen, P. E. (1973). In vitro chromosomal radiosensitivity in “chromosomal breakage syndromes”. *Cancer*, *32*(2), 380–383.

Hoch, N. C., Hanzlikova, H., Rulten, S. L., Tétreault, M., Komulainen, E., Ju, L., … Caldecott, K. W. (2017). XRCC1 mutation is associated with PARP1 hyperactivation and cerebellar ataxia. *Nature*, *541*(7635), 87–91.

Hoche, F., Seidel, K., Theis, M., Vlaho, S., Schubert, R., Zielen, S., & Kieslich, M. (2012).

Neurodegeneration in ataxia telangiectasia: what is new? What is evident? *Neuropediatrics*, *43*(3), 119–129.

Ito, K., Takubo, K., Arai, F., Satoh, H., Matsuoka, S., Ohmura, M., … Hirao, A. (2007). Regulation of reactive oxygen species by Atm is essential for proper response to DNA double-strand breaks in lymphocytes. *Journal of Immunology (Baltimore, Md. : 1950)*, *178*(1), 103–110.

Jakoby, W. B. (1978). The glutathione S-transferases: a group of multifunctional detoxification proteins. *Advances in Enzymology and Related Areas of Molecular Biology*, *46*, 383–414.

Kaiser, S. E., Riley, B. E., Shaler, T. A., Trevino, R. S., Becker, C. H., Schulman, H., & Kopito, R. R. (2011). Protein standard absolute quantification (PSAQ) method for the measurement of cellular ubiquitin pools. *Nature Methods*, *8*(8), 691–696.

Kamsler, A., Daily, D., Hochman, A., Stern, N., Shiloh, Y., Rotman, G., & Barzilai, A. (2001). Increased oxidative stress in ataxia telangiectasia evidenced by alterations in redox state of brains from Atm-deficient mice. *Cancer Research*, *61*(5), 1849–1854.

Khalil, H. ., Tummala, H., & Zhelev, N. (2012). ATM in focus: A damage sensor and cancer target. *Biodiscovery*, (5), 1.

Khoronenkova, S. V, & Dianov, G. L. (2015). ATM prevents DSB formation by coordinating SSB repair and cell cycle progression. *Proceedings of the National Academy of Sciences* , *112*(13), 3997–4002.

Kim, K., Biade, S., & Matsumoto, Y. (1998). Involvement of Flap Endonuclease 1 in Base Excision DNA Repair. *Journal of Biological Chemistry* , *273*(15), 8842–8848.

Kozlov, S. V, Waardenberg, A. J., Engholm-Keller, K., Arthur, J. W., Graham, M. E., & Lavin, M. (2016). Reactive Oxygen Species (ROS)-Activated ATM-Dependent Phosphorylation of Cytoplasmic Substrates Identified by Large-Scale Phosphoproteomics Screen. *Molecular & Cellular Proteomics : MCP*, *15*(3), 1032–1047.

Lakin, N. D., Weber, P., Stankovic, T., Rottinghaus, S. T., Taylor, A. M., & Jackson, S. P. (1996). Analysis of the ATM protein in wild-type and ataxia telangiectasia cells. *Oncogene*, *13*(12), 2707–2716.

Lavin, M. F., Gueven, N., Bottle, S., & Gatti, R. A. (2007). Current and potential therapeutic strategies for the treatment of ataxia-telangiectasia. *British Medical Bulletin*, *81–82*, 129–147.

Lecker, S. H., Goldberg, A. L., & Mitch, W. E. (2006). Protein Degradation by the Ubiquitin–Proteasome Pathway in Normal and Disease States. *Journal of the American Society of Nephrology* , *17*(7), 1807–1819.

Lee, J.-H., & Paull, T. T. (2005). ATM activation by DNA double-strand breaks through the Mre11-Rad50-Nbs1 complex. *Science (New York, N.Y.)*, *308*(5721), 551–554.

Lin, M. T., & Beal, M. F. (2006). Mitochondrial dysfunction and oxidative stress in neurodegenerative diseases. *Nature*, *443*(7113), 787–795.

Lindahl, T. (1993). Instability and decay of the primary structure of DNA. *Nature*, *362*(6422), 709–715.

Lindahl, T. (2000). Suppression of spontaneous mutagenesis in human cells by DNA base excision–repair. *Mutation Research/Reviews in Mutation Research*, *462*(2–3), 129–135.

Louis-Bar, D. (1941). Sur syndrome progressif comprenant des telangiectasies capillaires cutanees et

conjonctivales symetriques, a disposition naevoide et de troubles cerebelleux. *Confin Neurol (Basel)*, (4), 32–42.

Mann, M. (2006, December). Functional and quantitative proteomics using SILAC. *Nature Reviews. Molecular Cell Biology*. England.

Markkanen, E., Fischer, R., Ledentcova, M., Kessler, B. M., & Dianov, G. L. (2015). Cells deficient in base-excision repair reveal cancer hallmarks originating from adjustments to genetic instability. *Nucleic Acids Research*, *43*(7), 3667–3679.

Matsuoka, S., Rotman, G., Ogawa, A., Shiloh, Y., Tamai, K., & Elledge, S. J. (2000). Ataxia telangiectasia-mutated phosphorylates Chk2 in vivo and in vitro. *Proceedings of the National Academy of Sciences of the United States of America*, *97*(19), 10389–10394.

Maynard, S., Schurman, S. H., Harboe, C., de Souza-Pinto, N. C., & Bohr, V. A. (2009). Base excision repair of oxidative DNA damage and association with cancer and aging. *Carcinogenesis*, *30*(1), 2–10.

McKinnon, P. J. (2004). ATM and ataxia telangiectasia. *EMBO Reports*, *5*(8), 772–776.

McNeill, D. R., Narayana, A., Wong, H.-K., & Wilson, D. M. 3rd. (2004). Inhibition of Ape1 nuclease activity by lead, iron, and cadmium. *Environmental Health Perspectives*, *112*(7), 799–804.

Melvin, T., Botchway, S. W., Parker, A. W., & O'Neill, P. (1996). Induction of Strand Breaks in Single-Stranded Polyribonucleotides and DNA by Photoionization: One Electron Oxidized Nucleobase Radicals as Precursors. *Journal of the American Chemical Society*, *118*(42), 10031–10036.

Morgan, J. L., Holcomb, T. M., & Morrissey, R. W. (1968). Radiation reaction in ataxia telangiectasia. *American Journal of Diseases of Children (1960)*, *116*(5), 557–558.

Moyal, L., Lerenthal, Y., Gana-Weisz, M., Mass, G., So, S., Wang, S.-Y., … Shiloh, Y. (2011). Requirement of ATM-Dependent Monoubiquitylation of Histone H2B for Timely Repair of DNA Double-Strand Breaks. *Molecular Cell*, *41*(5), 529–542.

Nakamura, K., Kato, A., Kobayashi, J., Yanagihara, H., Sakamoto, S., Oliveira, D. V. N. P., … Komatsu, K. (2011). Regulation of homologous recombination by RNF20-dependent H2B ubiquitination. *Molecular Cell*, *41*(5), 515–528.

Natalia, S., Matthias, P., André, R., Thilo, D., Bendix, R., Skawran, B., & Stuhrmann, M. (1999). Characterization of ATM gene mutations in 66 ataxia telangiectasia families. *Human Molecular Genetics*, *8*(1), 69–79.

Nickson, C. M., & Parsons, J. L. (2014). Monitoring regulation of DNA repair activities of cultured cells in-gel using the comet assay . *Frontiers in Genetics.*

Nowak-Wegrzyn, A., Crawford, T. O., Winkelstein, J. A., Carson, K. A., & Lederman, H. M. (2004). Immunodeficiency and infections in ataxia-telangiectasia. *The Journal of Pediatrics*, *144*(4), 505–511.

Nowak, R. (1995). Discovery of AT gene sparks biomedical research bonanza. *Science*, *268*(5218), 1700 LP-1701.

Oda, Y., Huang, K., Cross, F. R., Cowburn, D., & Chait, B. T. (1999). Accurate quantitation of protein expression and site-specific phosphorylation. *Proceedings of the National Academy of Sciences* , *96*(12), 6591–6596.

Ong, S.-E., Blagoev, B., Kratchmarova, I., Kristensen, D. B., Steen, H., Pandey, A., & Mann, M. (2002). Stable isotope labeling by amino acids in cell culture, SILAC, as a simple and accurate approach to expression proteomics. *Molecular & Cellular Proteomics : MCP*, *1*(5), 376–386.

Orlando, G., Khoronenkova, S. V, Dianova, I. I., Parsons, J. L., & Dianov, G. L. (2014). ARF induction in response to DNA strand breaks is regulated by PARP1. *Nucleic Acids Research*, *42*(4), 2320–2329.

Parsons, J. L., Tait, P. S., Finch, D., Dianova, I. I., Edelmann, M. J., Khoronenkova, S. V, … Dianov, G. L. (2009). Ubiquitin ligase ARF-BP1/Mule modulates base excision repair. *The EMBO Journal*, *28*(20), 3207–3215.

Paull, T. T. (2015). Mechanisms of ATM Activation. *Annual Review of Biochemistry*, *84*, 711–738.

Pellom, S. T., & Shanker, A. (2012). Development of Proteasome Inhibitors as Therapeutic Drugs. *Journal of Clinical & Cellular Immunology*, *Suppl 5*, 5.

Poletto, M., Legrand, A. J., Fletcher, S. C., & Dianov, G. L. (2016). p53 coordinates base excision repair to prevent genomic instability. *Nucleic Acids Research*, *44*(7), 3165–3175.

Reichenbach, J., Schubert, R., Schindler, D., Muller, K., Bohles, H., & Zielen, S. (2002). Elevated oxidative stress in patients with ataxia telangiectasia. *Antioxidants & Redox Signaling*, *4*(3), 465–469.

Reichenbach, J., Schubert, R., Schwan, C., Müller, K., Böhles, H. J., & Zielen, S. (1999). Anti-oxidative capacity in patients with ataxia telangiectasia. *Clinical and Experimental Immunology*, *117*(3), 535–539.

Robertson, A. B., Klungland, A., Rognes, T., & Leiros, I. (2009). DNA repair in mammalian cells: Base excision repair: the long and short of it. *Cellular and Molecular Life Sciences : CMLS*, *66*(6), 981–993.

Rothblum-Oviatt, C., Wright, J., Lefton-Greif, M. A., McGrath-Morrow, S. A., Crawford, T. O., & Lederman, H. M. (2016). Ataxia telangiectasia: a review. *Orphanet Journal of Rare Diseases*, *11*(1), 159.

Rotman, G., & Shiloh, Y. (1997). Ataxia-telangiectasia: is ATM a sensor of oxidative damage and stress? *BioEssays : News and Reviews in Molecular, Cellular and Developmental Biology*, *19*(10), 911–917.

Savitsky, K., Bar-Shira, A., Gilad, S., Rotman, G., Ziv, Y., Vanagaite, L., … Shiloh, Y. (1995). A single ataxia telangiectasia gene with a product similar to PI-3 kinase. *Science (New York, N.Y.)*, *268*(5218), 1749–1753.

Schieber, M., & Chandel, N. S. (2014). ROS function in redox signaling and oxidative stress. *Current Biology : CB*, *24*(10), R453-62.

Schmahmann, J. D. (2004). Disorders of the cerebellum: ataxia, dysmetria of thought, and the cerebellar cognitive affective syndrome. *The Journal of Neuropsychiatry and Clinical Neurosciences*, *16*(3), 367–378.

SEDGWICK, R. P., & BODER, E. (1960). Progressive ataxia in childhood with particular reference to ataxia-telangiectasia. *Neurology*, *10*, 705–715.

Seeberg, E., Eide, L., & Bjoras, M. (1995). The base excision repair pathway. *Trends in Biochemical*

Sciences, *20*(10), 391–397.

Shiloh, Y. (2003). ATM and related protein kinases: safeguarding genome integrity. *Nature Reviews. Cancer*, *3*(3), 155–168.

Shiloh, Y., & Kastan, M. B. (2001). ATM: genome stability, neuronal development, and cancer cross paths. *Advances in Cancer Research*, *83*, 209–254.

Shiloh, Y., & Ziv, Y. (2013). The ATM protein kinase: regulating the cellular response to genotoxic stress, and more. *Nat Rev Mol Cell Biol*, *14*(4), 197–210.

Sordet, O., Redon, C. E., Guirouilh-Barbat, J., Smith, S., Solier, S., Douarre, C., … Pommier, Y. (2009). Ataxia telangiectasia mutated activation by transcription- and topoisomerase I-induced DNA double-strand breaks. *EMBO Reports*, *10*(8), 887 LP-893.

Stracker, T. H., Roig, I., Knobel, P. A., & Marjanovic, M. (2013). The ATM signaling network in development and disease. *Frontiers in Genetics*, *4*, 37.

Sun, X., Becker-Catania, S. G., Chun, H. H., Hwang, M. J., Huo, Y., Wang, Z., … Gatti, R. A. (2002). Early diagnosis of ataxia-telangiectasia using radiosensitivity testing. *The Journal of Pediatrics*, *140*(6), 724–731.

Sung, J.-S., & Demple, B. (2006). Roles of base excision repair subpathways in correcting oxidized abasic sites in DNA. *FEBS Journal*, *273*(8), 1620–1629.

Suzuki, Y. J., Carini, M., & Butterfield, D. A. (2010). Protein Carbonylation. *Antioxidants & Redox Signaling*, *12*(3), 323–325.

Swift, M., Morrell, D., Cromartie, E., Chamberlin, A. R., Skolnick, M. H., & Bishop, D. T. (1986). The incidence and gene frequency of ataxia-telangiectasia in the United States. *American Journal of Human Genetics*, *39*(5), 573–583.

Syllaba, L., & Henner, K. (1926). Contribution a l'independance de l'athetose double idiopathique et congenitale. *Rev Neurol (Paris)*, (1), 541–562.

Tanaka, M., Lai, J. S., & Herr, W. (1992). Promoter-selective activation domains in Oct-1 and Oct-2 direct differential activation of an snRNA and mRNA promoter. *Cell*, *68*(4), 755–767.

Tyedmers, J., Mogk, A., & Bukau, B. (2010). Cellular strategies for controlling protein aggregation. *Nat Rev Mol Cell Biol*, *11*(11), 777–788.

Uttara, B., Singh, A. V, Zamboni, P., & Mahajan, R. T. (2009). Oxidative Stress and Neurodegenerative Diseases: A Review of Upstream and Downstream Antioxidant Therapeutic Options. *Current Neuropharmacology*, *7*(1), 65–74.

Valentin-Vega, Y. A., MacLean, K. H., Tait-Mulder, J., Milasta, S., Steeves, M., Dorsey, F. C., … Kastan, M. B. (2012a). Mitochondrial dysfunction in ataxia-telangiectasia. *Blood*, *119*(6), 1490–1500.

Valentin-Vega, Y. A., MacLean, K. H., Tait-Mulder, J., Milasta, S., Steeves, M., Dorsey, F. C., … Kastan, M. B. (2012b). Mitochondrial dysfunction in ataxia-telangiectasia. *Blood*, *119*(6), 1490–1500.

van Gent, D. C., Hoeijmakers, J. H., & Kanaar, R. (2001). Chromosomal stability and the DNA double-stranded break connection. *Nature Reviews. Genetics*, *2*(3), 196–206.

Voges, D., Zwickl, P., & Baumeister, W. (1999). The 26S proteasome: a molecular machine designed for controlled proteolysis. *Annual Review of Biochemistry*, *68*, 1015–1068.

Winterbourn, C. C. (2013). The biological chemistry of hydrogen peroxide. *Methods in Enzymology*, *528*, 3–25.

Wojewodzka, M., Buraczewska, I., & Kruszewski, M. (2002). A modified neutral comet assay: elimination of lysis at high temperature and validation of the assay with anti-single-stranded DNA antibody. *Mutation Research*, *518*(1), 9–20.